1996

Design and performance of the Moss Landing Marine Laboratories / Martek beam transmissometer

Joseph Andrew Gashler
San Jose State University

INFORMATION TO USERS

This manuscript has been reproduced from the microfilm master. UMI films the text directly from the original or copy submitted. Thus, some thesis and dissertation copies are in typewriter face, while others may be from any type of computer printer.

The quality of this reproduction is dependent upon the quality of the copy submitted. Broken or indistinct print, colored or poor quality illustrations and photographs, print bleedthrough, substandard margins, and improper alignment can adversely affect reproduction.

In the unlikely event that the author did not send UMI a complete manuscript and there are missing pages, these will be noted. Also, if unauthorized copyright material had to be removed, a note will indicate the deletion.

Oversize materials (e.g., maps, drawings, charts) are reproduced by sectioning the original, beginning at the upper left-hand corner and continuing from left to right in equal sections with small overlaps. Each original is also photographed in one exposure and is included in reduced form at the back of the book.

Photographs included in the original manuscript have been reproduced xerographically in this copy. Higher quality 6" x 9" black and white photographic prints are available for any photographs or illustrations appearing in this copy for an additional charge. Contact UMI directly to order.

UMI

A Bell & Howell Information Company
300 North Zeeb Road, Ann Arbor MI 48106-1346 USA
313/761-4700 800/521-0600

DESIGN AND PERFORMANCE OF THE MOSS LANDING MARINE LABORATORIES/MARTEK BEAM TRANSMISSOMETER

A Thesis

Presented to

The Faculty of Moss Landing Marine Laboratories

San Jose State University

In Partial Fulfillment of the Requirements for the Degree

Master of Science

By

Joseph Andrew Gashler

December 1996

APPROVED FOR MOSS LANDING MARINE LABORATORIES

Dr. William W. Broenkow

Dr. H. Sarma Lakkaraju

Dr. Nicholas A. Welschmeyer

APPROVED FOR THE UNIVERSITY

Abstract

DESIGN AND PERFORMANCE OF THE MOSS LANDING MARINE LABORATORIES/MARTEK BEAM TRANSMISSOMETER

by Joseph Andrew Gashler

Scattering of light by particles in natural waters is wavelength dependent, with blue wavelengths being scattered more strongly than red. A transmissometer designed for maximum sensitivity to particles will use a blue beam of light. A Martek XMS beam transmissometer was modified to use an AC modulated blue LED as its source. Synchronous detectors at the end of optical and reference paths were used to calculate transmittance. The performance of the modified instrument was assessed through a variety of field and laboratory tests. The MLML/Martek transmissometer demonstrated a precision of 0.06 % , accuracy to within 0.004 m^{-1} of published values for pure water, and stability with respect to temperature equivalent to 0.2 % over a temperature range of 5 to 20 degrees C. The new design proved 3.7 times more sensitive to the observed range of turbidities than a popular production transmissometer in side by side testing in Monterey Bay.

Acknowledgements

This research was supported by Dennis Clark of the National Oceanic and Atmospheric Administration via National Environmental Satellite Data Information Service Grant No. NA17EC0428 to Dr. William Broenkow. I also received financial support from the Dr. Earl H. and Ethel M. Myers Oceanographic and Marine Biology Trust. Dr. Sarma Lakkaraju of San Jose State University designed the electronics tested in this study, and his counsel and guidance through out the instrument development is greatly appreciated. John Arvesen and Robert Wrigley of NASA Ames Research Center supplied the original version of the Martek XMS transmissometer to Moss Landing Marine Laboratories. Drs. Nick Welschmeyer, Alissa Arp, and Ken Bruland generously allowed us to test our instrument during their cruises. Rich Muller performed data acquisition at sea aboard the *R/V Point Sur.*

Beyond these formal contributions I wish to acknowledge the faculty and staff of the Moss Landing Marine Laboratories, and in particular major advisor Dr. William Broenkow. Dr. Sarma Lakkaraju of San Jose State University and Dr. Nicholas Welschmeyer of Moss Landing Marine Labs served as thesis committee members, and I appreciate their comments and constructive criticism. Gail Johnston provided crucial administrative support throughout my research. Sandy and Mark Yarbrough provided humor, inspiration, and invaluable technical advice. I appreciate the good will and tolerance of my shipmates in the physical oceanography lab and at NOAA. To all of these people I am deeply indebted, and I wish them the best.

It goes without saying that all of these contributions would be for naught without the support of family and friends.

Contents

List of Figures

Figure **Page**

Figure **Page**

Introduction

Beam attenuation is one of the most important physical properties that is used to characterize the bio-optical state of natural waters. The attenuation coefficient has been used to provide a measure of total suspended material (eg. Bishop, 1986; Pak *et al.*, 1988; Spinrad *et al.*, 1989; Broenkow *et al.*, 1992); the inverse of the beam attenuation coefficient is important as a scaling parameter for problems in imaging and radiative transfer (Voss, 1992); and the chlorophyll-specific beam attenuation coefficient has been used to classify waters for the purposes of assessment via remote sensing (Mitchell and Holm-Hansen, 1991). The profile of beam attenuation, combined with those of chlorophyll fluorescence and dissolved oxygen, is of interest to the biological oceanographer who seeks information regarding the vertical structure of phytoplankton in the upper ocean.

The beam attenuation coefficient is measured by the beam transmissometer, an instrument which projects a beam of light through the water and measures its intensity at the end of a known optical path. Different combinations of optical and electronic designs have been employed to achieve this end. Transmissometers have been deployed on moorings, in towed or flow-through configurations aboard ships, on remotely operated vehicles (ROV), and on conductivity-temperature-depth (CTD) profilers.

Early transmissometer designs include that developed by Petzold and Austin

(1968) at the Visibility Laboratory of the Scripps Institute of Oceanography, a production version of which became the Martek XMS transmissometer, and a design developed by Bartz *et al.* (1978) which later became the Sea Tech transmissometer. The physical oceanography group at Moss Landing Marine Laboratories built a 2000 meter pressure housing for a Martek XMS transmissometer with which they made one of the early sets of deep transmissometer measurements in the eastern tropical Pacific (Broenkow *et al.*, 1983) as part of the VERTEX project (Martin *et al.*, 1983). It is this instrument that was further modified in this study.

The modified Martek transmissometer will be used by the MLML physical oceanography group at the Marine Optical BuoY (MOBY) mooring site (20° 48.96' N, 157° 00.81' W) 10 nautical miles to the lee of the Hawaiian island of Lanai as part of the continuing Marine Optical Characterization Experiments (MOCE) associated with future ocean color satellites SeaWiFS and MODIS. Beam attenuation at 490 nm in the area of interest ranges from 0.02 to 0.04 m^{-1} (Feinholz et al., 1995b) -- attenuation similar to that of pure water (0.0227 m^{-1} at 490 nm) (Smith and Baker, 1981). Secchi depths in this area approach 40 meters. A transmissometer optimized for these conditions is one that accurately measures the beam attenuation coefficient of very clear water.

Sensitivity of the transmissometer to particles is a priority in these conditions. Particles in water scatter blue light more than red (Gordon and Morel, 1983); a blue source was chosen for the new design. Other investigators have chosen to measure beam attenuation in the red end of the spectrum to avoid the effects of dissolved organic matter,

which absorbs more strongly in the blue end of the spectrum, but these effects are small in the open ocean where concentration of dissolved organic matter is low. To avoid the high current requirements and breakable filaments of incandescent bulbs, a blue light emitting diode (LED) was used as the source. The LED was modulated and synchronous detectors were used to eliminate errors caused by ambient photons scattered into the field of view of the detector.

The performance of the modified Martek instrument was assessed through a variety of laboratory and field tests designed to characterize its accuracy, precision, sensitivity to particle concentration, and stability with respect to temperature. To compare its precision and sensitivity under field conditions with that of a widely used instrument it was tested side by side with the Sea Tech 25 cm path transmissometer. Sea trials consisted of a total of 46 casts during June and July 1996 off the central California coast. The initial characterization of the performance of the modified Martek instrument is presented here.

Background

Attenuation of light in water is governed by the processes of absorption and scattering. Absorption of light is the transformation of photons into thermal or chemical energy; scattering is a random process by which photons are redirected without losing energy. The coefficients that quantify these processes are independent of the ambient

light field and are thus termed "inherent" properties of the water. Of the three inherent optical properties of water -- absorption, scattering, and attenuation -- it is beam attenuation that is the most easily and reliably measured.

Attenuation of light over a path length z in water is described to first order by the differential equation:

$$\frac{dI}{dz} = -cI$$

where I is the intensity of the light and c is the attenuation coefficient. We integrate to find that the propagation of light is described by the equation:

$$I(z) = I(0)e^{-cz} \qquad (1)$$

By measuring the intensity of a monochromatic beam of light at two ends of a known path length, the beam attenuation coefficient c can be calculated from:

$$c = \left(-\frac{1}{z}\right)\ln\left(\frac{I(z)}{I(0)}\right) \qquad (2)$$

This is in principle a straightforward measurement, but "there are some pitfalls to be avoided if the measurement is to be truly meaningful" (Petzold and Austin, 1968). Careful calibrations must be diligently performed if accurate values of the attenuation coefficient are to be obtained.

The attenuation coefficient (c) is the sum of the total absorption coefficient (a) and total scattering coefficient (b).

$$c(\lambda) = a(\lambda) + b(\lambda) \tag{3}$$

The absorption and scattering coefficients can be further subdivided into components corresponding to pure water, chlorophyll, particles, and dissolved organic material (Mobley, 1994).

$$a_{total}(\lambda) = a_{water}(\lambda) + a_{chl}(\lambda) + a_{dissolved}(\lambda)$$

$$b_{total}(\lambda) = b_{water}(\lambda) + b_{particles}(\lambda)$$

Figure 1 shows the spectral attenuation of pure water from 400 to 700 nm as measured by Smith and Baker (1981). The attenuation of pure water at the wavelengths of the transmissometers used in this study are marked and labelled.

Morel (1991) gives a parameterized form of the model of Prieur and Sathyendranath (1981) for the absorption due to chlorophyll as:

$$a_{chl}(\lambda) = 0.06 a_c^*(\lambda) [chl]^{0.65} (1+0.2e^{-0.014(\lambda-440)}) \tag{4}$$

where the chlorophyll specific absorption coefficient $a_c^*(\lambda)$ in m^2mg^{-1} is given in table 2 of Prieur and Sathyendranath (1981) and the chlorophyll concentration [chl] is in mg m^{-3}.

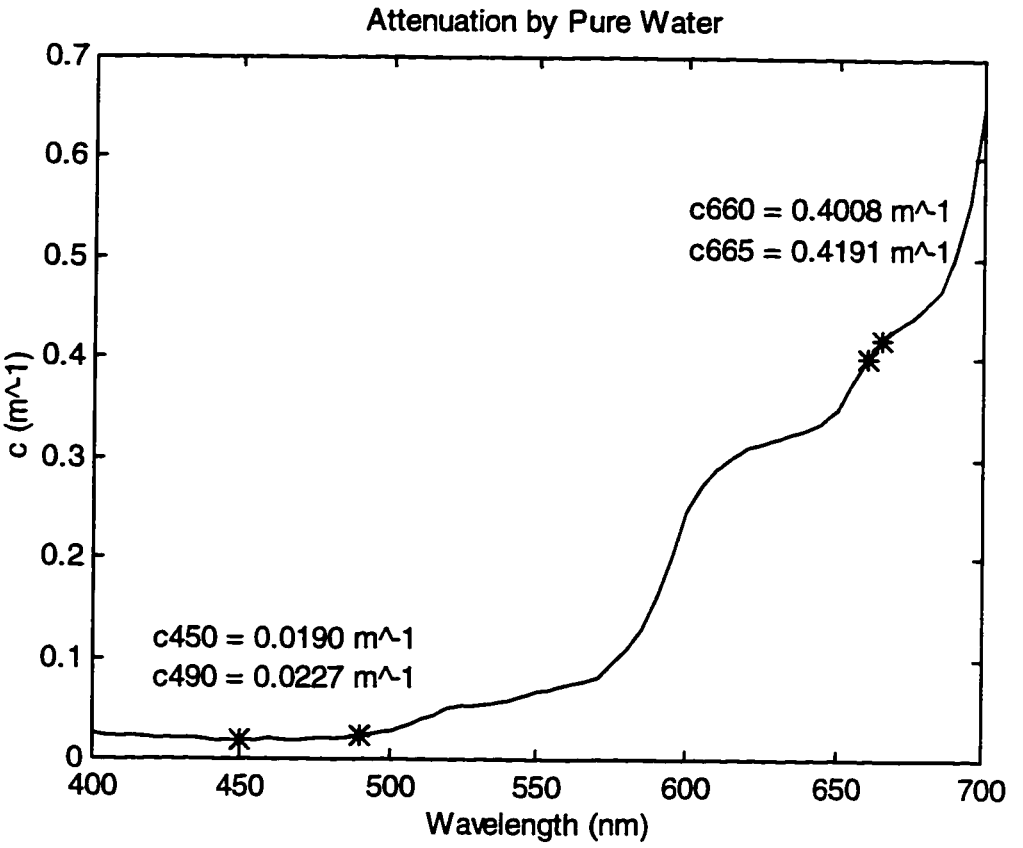

Figure 1. The spectrum of attenuation of pure water from 400 to 700 nm as measured by Smith and Baker (1981). The attenuation coefficients of pure water at the source wavelengths of transmissometers used in this study are marked and labelled.

The units of a are m^{-1}. Figure 2 shows the absorption coefficient of chlorophyll from 400 to 700 nm for chlorophyll concentrations ranging from 0.1 to 5.0 mg m^{-3}. The exponential term on the right hand side of equation 4 contains the implicit assumption that there will be some dissolved organic material that covaries with chlorophyll concentration and contributes to the total absorption spectra. "Chlorophyll concentration" refers here to the sum of chlorophyll a, the main photosynthetic pigment in phytoplankton, and the product of its breakdown, pheophytin a.

The scattering coefficient of particles can be derived from the volume scattering function, which is in turn calculated from Mie theory. Particle concentration, size, and relative index of refraction all affect the scattering coefficient. In practice detailed knowledge of these particle properties is lacking, but an estimate of the total scattering coefficient can be obtained for the open ocean from an equation given by Gordon and Morel (1983):

$$b(\lambda) = \left(\frac{550}{\lambda}\right) 0.30 [chl]^{0.62} \qquad (5)$$

Here the units of chlorophyll concentration [chl] are mg m^{-3}, the units of wavelength are nm, and those of b are m^{-1}. Figure 3 shows the spectral scattering coefficient of natural water from 400 to 700 nm for chlorophyll concentrations ranging from 0.1 to 5.0 mg m^{-3}.

Dissolved organic matter forms a class of substances described as humic substances, which are classified according to solubility (Kirk, 1983). The material which

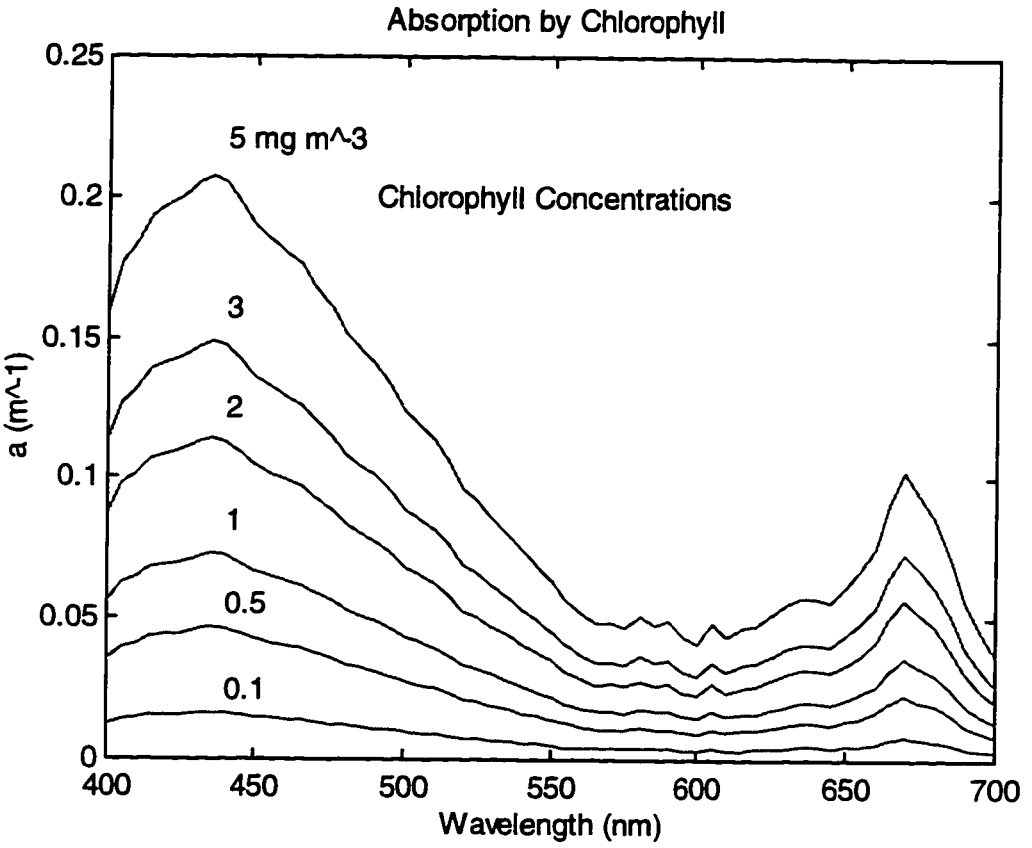

Figure 2. Spectra of chlorophyll absorption from 400 to 700 nm as modeled by Prieur and Sathyendranath (1981) for chlorophyll concentrations from 0.1 to 5.0 mg m^{-3}.

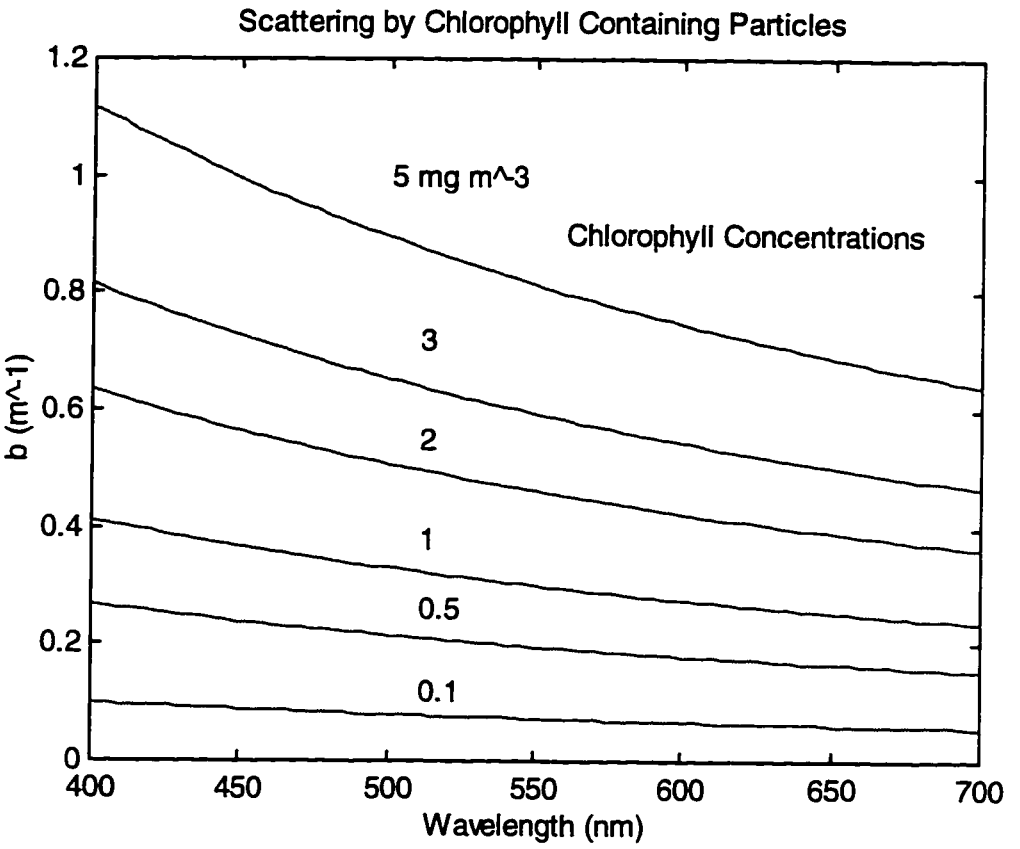

Figure 3. The spectral scattering coefficient of natural water from 400 to 700 nm as modeled by Gordon and Morel (1983) for chlorophyll concentrations ranging from 0.1 to 5.0 mg m^{-3}.

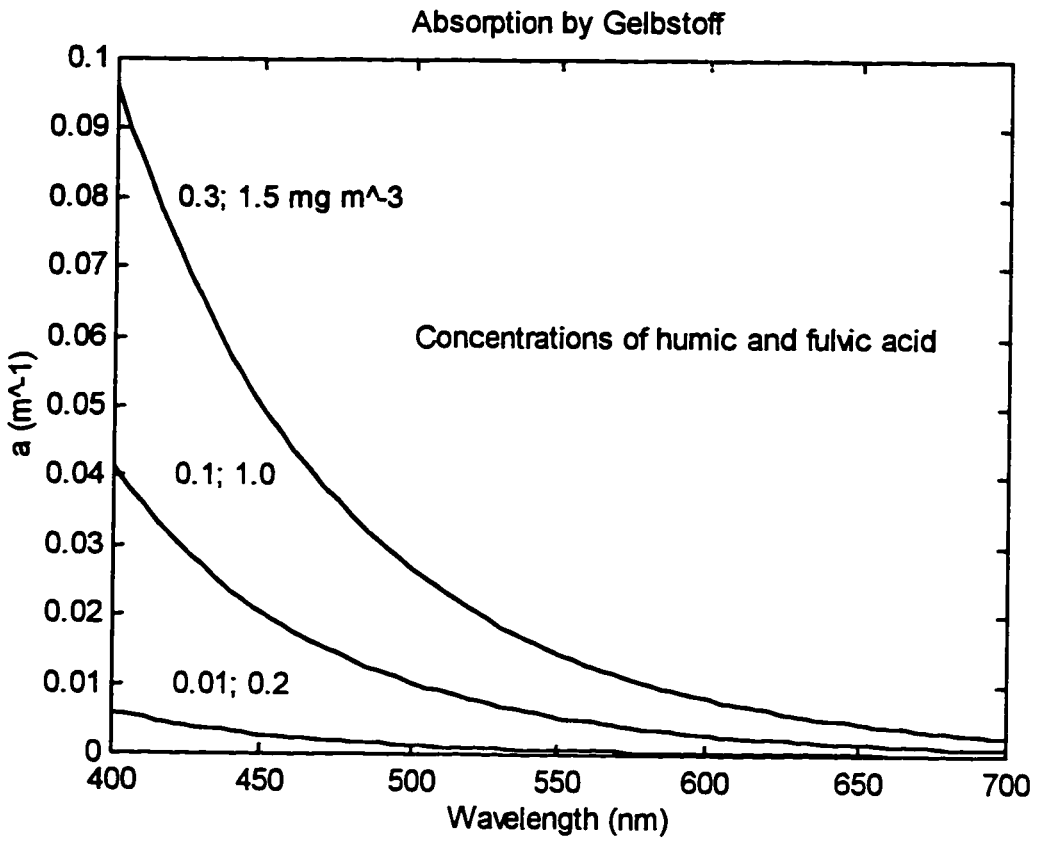

Figure 4. The spectral absorption of dissolved organic material from 400 to 700 nm for concentrations typical of coastal and oligotrophic conditions. The range of concentrations of fulvic acid are from 0.2 to 1.5 mg m^{-3}, and of humic acid from 0.01 to 0.3 mg m^{-3}.

dissolves in alkali is known as humin. Of that which remains, the fraction which precipitates upon acidification is called humic acid; the fraction which does not is called fulvic acid. Carder *et al.* (1989) modeled the absorption of dissolved organic matter by considering separately the contribution of marine humic and fulvic acids.

$$a_{dissolved}(\lambda) = [fulvic]\, a_f^* e^{(S_f(450-\lambda))} + [humic]\, a_h^* e^{(S_h(450-\lambda))} \qquad (6)$$

where $S_f = 0.019$ nm^{-1}, $S_h = 0.011$ nm^{-1}, the mass specific absorption coefficients are $a^*_f = 0.0073$ m^2 mg^{-1}, $a^*_h = 0.13$ m^2 mg^{-1} and the concentrations of fulvic and humic acid are in mg m^{-3}. Figure 4 shows the absorption of this "yellow substance" for concentrations typical of coastal and oligotrophic conditions. The range of concentrations of fulvic acid are from 0.2 to 1.5 mg m^{-3}, and of humic acid from 0.01 to 0.3 mg m^{-3}. Examination of the scales of figures 1 through 4 shows that dissolved organic matter plays a relatively small role in total attenuation in typical marine environments. The exception is regions subject to significant terrestrial runoff, which may introduce large concentrations dissolved organic material.

The relative contributions of absorption and scattering to total attenuation are functions of chlorophyll concentration. At the low concentrations (0.1 mg m^{-3}) of chlorophyll typical of the open ocean the total attenuation spectrum is dominated by the absorption of the water itself (figure 5). At the moderate concentrations (1.0 mg m^{-3}) of chlorophyll typical of coastal waters the scattering of particles and absorption of pure

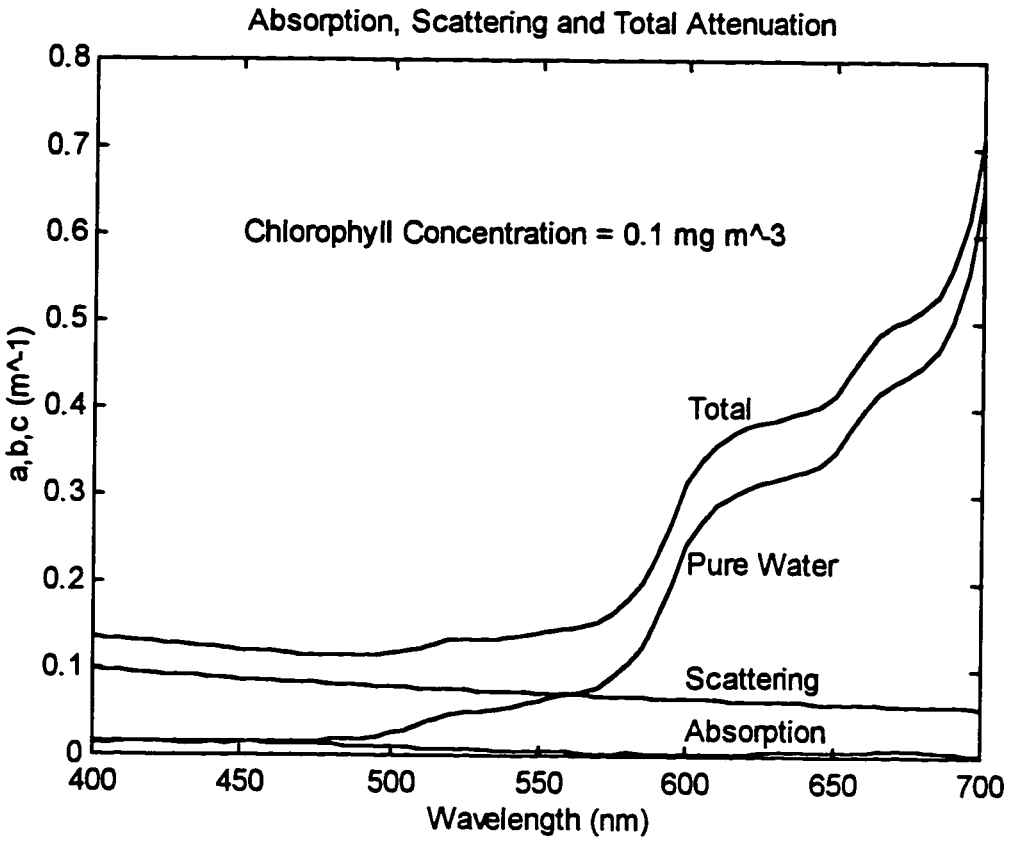

Figure 5. The contributions of chlorophyll absorption, chlorophyll scattering, and pure water to total attenuation for low chlorophyll concentrations.

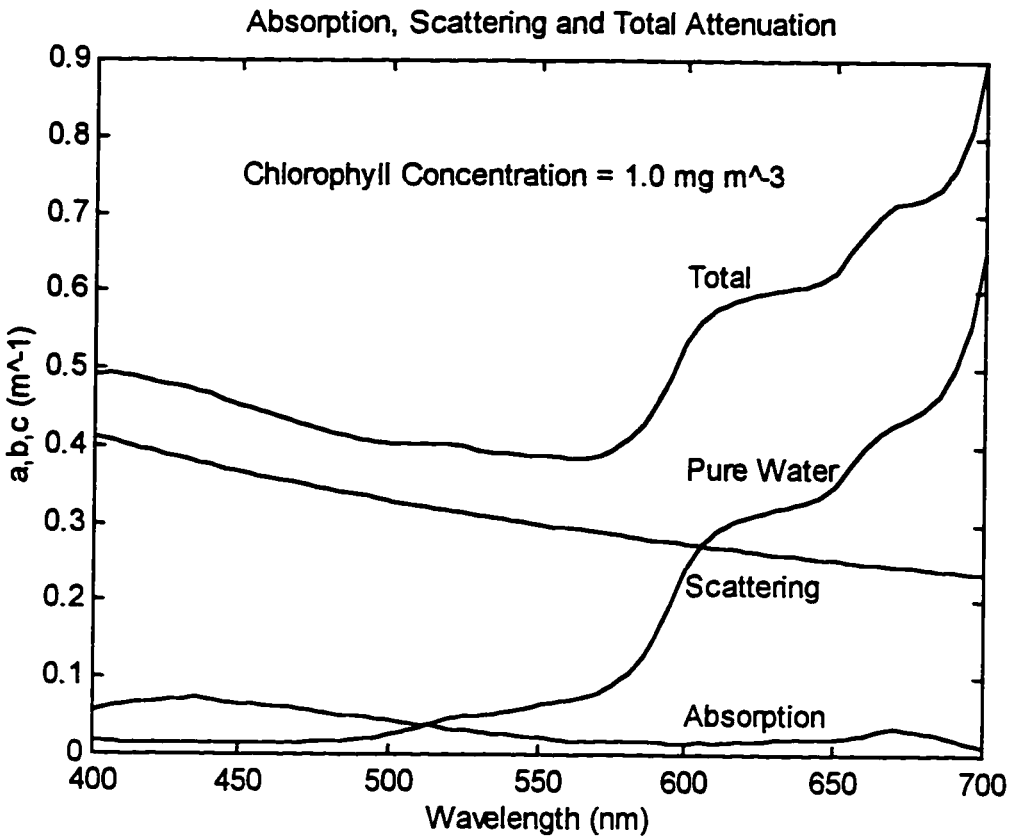

Figure 6. The contributions of chlorophyll absorption, chlorophyll scattering, and pure water to total attenuation for moderate concentrations of chlorophyll.

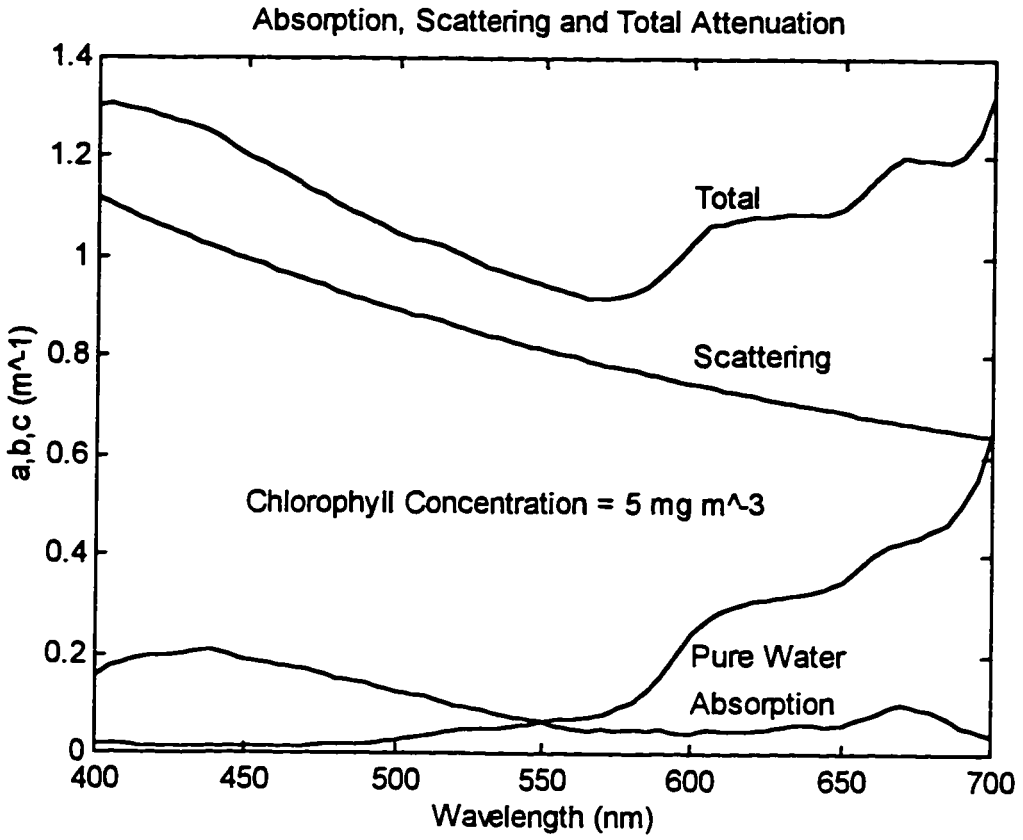

Figure 7. The contributions of chlorophyll absorption, chlorophyll scattering, and pure water to total attenuation for high concentrations of chlorophyll.

water are comparable, and the absorption of chlorophyll is greater than that of pure water in the blue part of the spectrum but not in the red (figure 6). At high (5 mg m^{-3}) concentrations of chlorophyll the spectrum of total attenuation is dominated by scattering (figure 7). We have considered only the contributions of phytoplankton and their derivatives, thus this analysis is only valid for Case 1 waters (Morel and Prieur, 1977), not those containing significant concentrations of particles of abiotic origin.

The spectra of attenuation due to particles (total attenuation minus that of pure water) are those which are of interest to an oceanographer who seeks to make inferences regarding particle concentrations from optical data. The attenuation due to particles is always higher in the blue end of the spectrum than in the red, and the effect is more pronounced at higher concentrations of particles (figure 8). A transmissometer designed for maximum sensitivity to particles will use a blue beam of light.

Optical Considerations

An accurate transmissometer will detect neither scattered photons nor those of any other origin than the transmissometer source. The detection of photons which are scattered into the field of view of the detector will cause erroneously low values of beam attenuation. Two optical schemes have evolved which employ imaging optics to achieve this end: the collimated optical system and the cylindrically limited system (figures 9 and 10). The two systems use almost identical components; the main difference between the

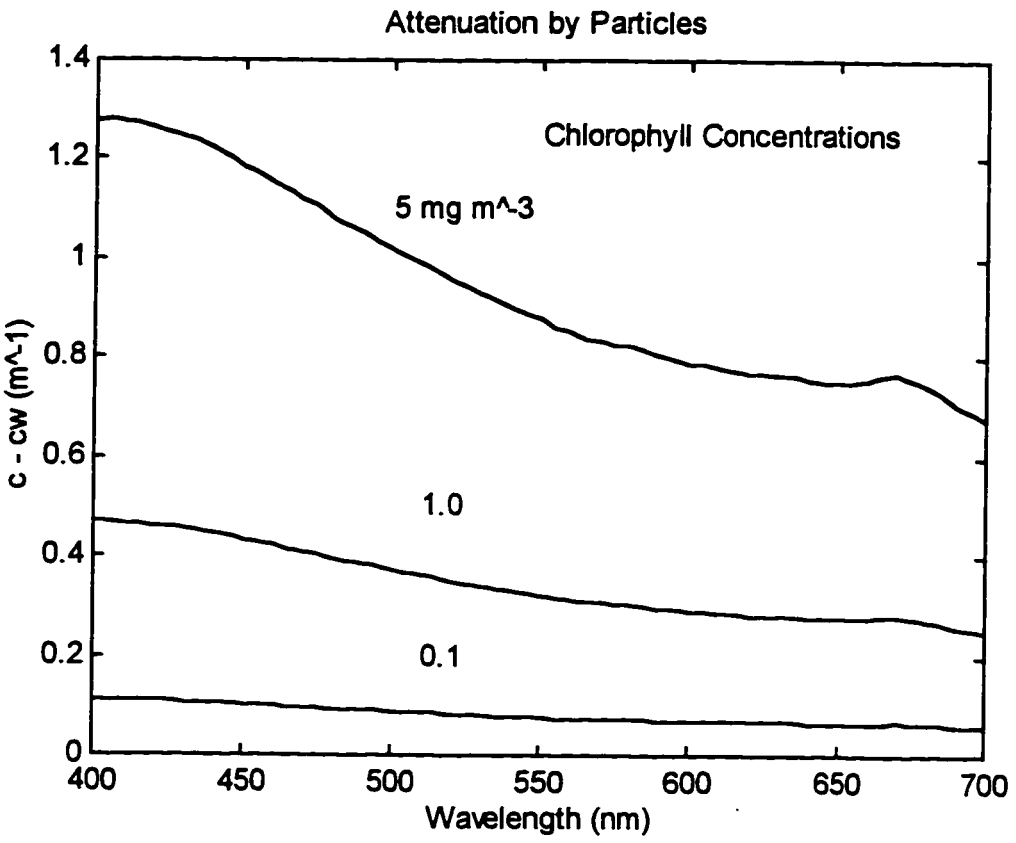

Figure 8. The spectra of attenuation due to particles (total attenuation minus that of pure water) for chlorophyll concentrations of 0.1, 1.0, and 5.0 mg m^{-3}.

Collimated Optical System

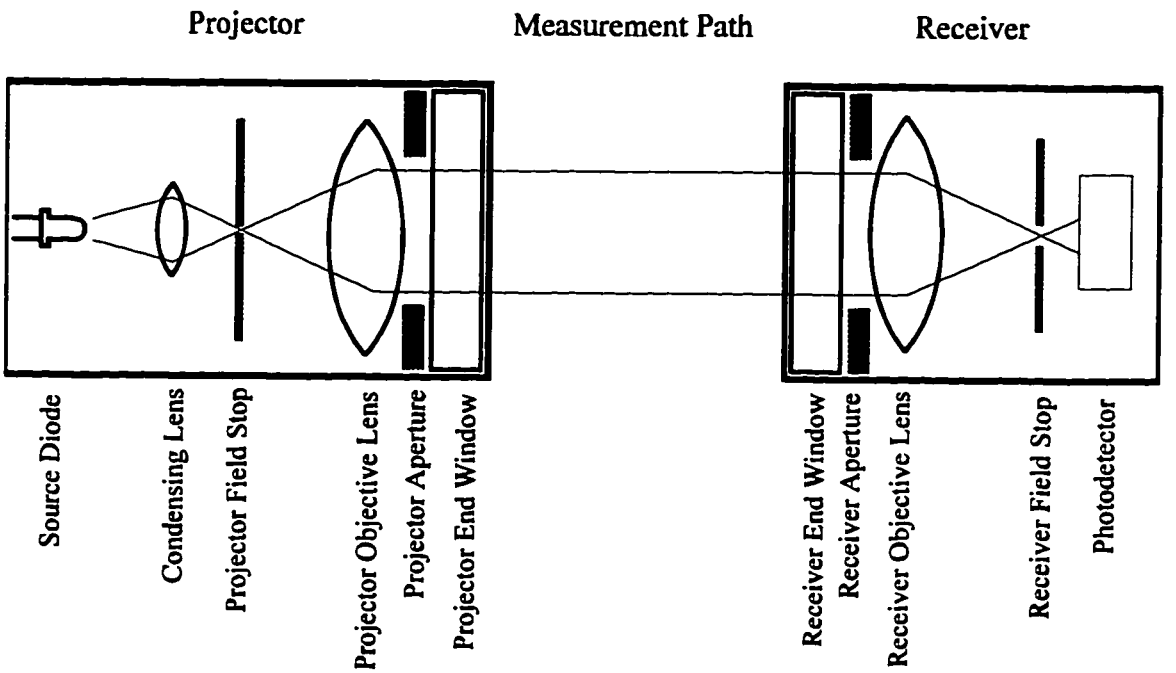

Figure 9. The collimated optical system for measuring the beam attenuation coefficient. The Sea Tech 25 cm path transmissometer uses a collimated system.

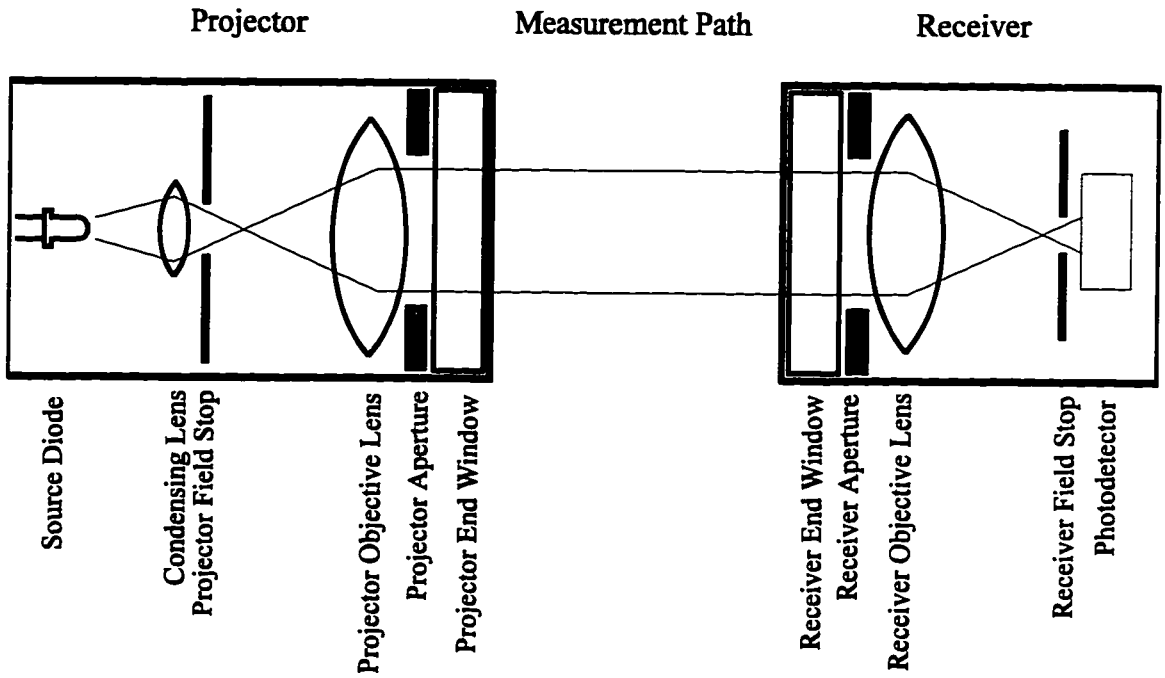

Figure 10. The cylindrically limited optical system for measuring the beam attenuation coefficient. The Martek XMS and modified Martek transmissometers use a cylindrically limited system.

two is that in the collimated optical system all the rays of light in the beam are parallel whereas in a cylindrically limited system the measurement path is traversed by all rays which can be drawn between the projector and receiver apertures. The explanation of the two systems below follows that of Austin and Petzold (1977).

Both optical systems consist of a projector and a receiver, with the projector containing the light source and its associated optics and the receiver containing the photodetector and its associated optics. A prism or mirrors may be used to fold the path, which increases the length of the optical path and has the added advantage of allowing the projector and receiver optics and electronics to be placed in the same watertight housing.

In the collimated system (figure 9) the projector consists of a light source, a condensing lens which images the light source at the field stop, and an objective lens which images the source at infinity. The projector field stop is located in the focal plane of the projector objective lens. A beam of light is formed which leaves the projector and diverges with a half-angle described by:

$$\gamma = \frac{D}{2f} \tag{7}$$

where D is the diameter of the field stop and f is the focal length of the projector's objective lens. This beam passes through the projector aperture and end window and travels the length of the optical path where it reaches the receiver.

At the receiver the beam passes through an end window and aperture, where it reaches the objective lens of the receiver. The objective lens forms an image of the source at the field stop which is located in its focal plane. This field stop together with the objective lens restricts the field of view of the detector according to equation 7 above. The optical path ends with a photodetector located behind the field stop.

The cylindrically limited optical system (figure 10) also consists of a projector and a receiver. As in the collimated system the condensing lens in the projector forms an image of the source at the projector field stop. The projector's objective lens forms an image, in air, of the projector field stop at the receiver aperture. The field stop in the cylindrically limited system is located between the source and the focal plane of the projector objective lens. The field stop is of such a size that its image is the same size as the receiver aperture. The beam is composed, not of parallel rays, but of all rays which lie between the projector and receiver apertures.

The receiver objective lens forms an image, *in water*, of the receiver field stop at the aperture of the projector. It is important that the objective lens and field stop be located such that the entire projector aperture is imaged at the receiver field stop when the instrument is submerged. If the projector aperture is imaged at the receiver field stop in air, then upon submersion in a medium of different index of refraction the aperture would be imaged past the field stop and its edges would be clipped, resulting in erroneously low values of transmittance.

One difference between the two systems is the amount of tolerance that each has

for a given amount of mechanical instability in the optical path. Deflection of the two parallel end windows will cause the beam of either system to be focused at a different point in the focal plane of the receiver objective lens, but this refocusing has different implications for accuracy in each case. Errors caused by mechanical instability are illustrated by figure 11.

In the case of the collimated beam system, an angular deflection of θ causes the beam to be focused at a point located a distance $f\theta$ off-axis, in the focal plane of the lens. If the distance $f\theta$ is larger than the radius of the receiver field stop then the beam will focused outside the field stop and none of the photons from the source will reach the detector. The error in transmittance will therefore be 100% for an angular deflection greater than that expressed by:

$$\theta_{max,col} = \frac{d_{col}}{f}$$

where d_{col} is the radius of the collimated system's receiver field stop and f is the focal length of the lens.

The error due to the same angular deflection in a cylindrically limited system will be less than 100 percent. The error in a cylindrically limited system can be approximated by calculating the percentage of the beam which will be clipped by the receiver field stop for a given angular deflection. By calculating the percentage clipped for an angular deflection equal to d_{col}/f -- the angular deflection which produced an error of 100% in the

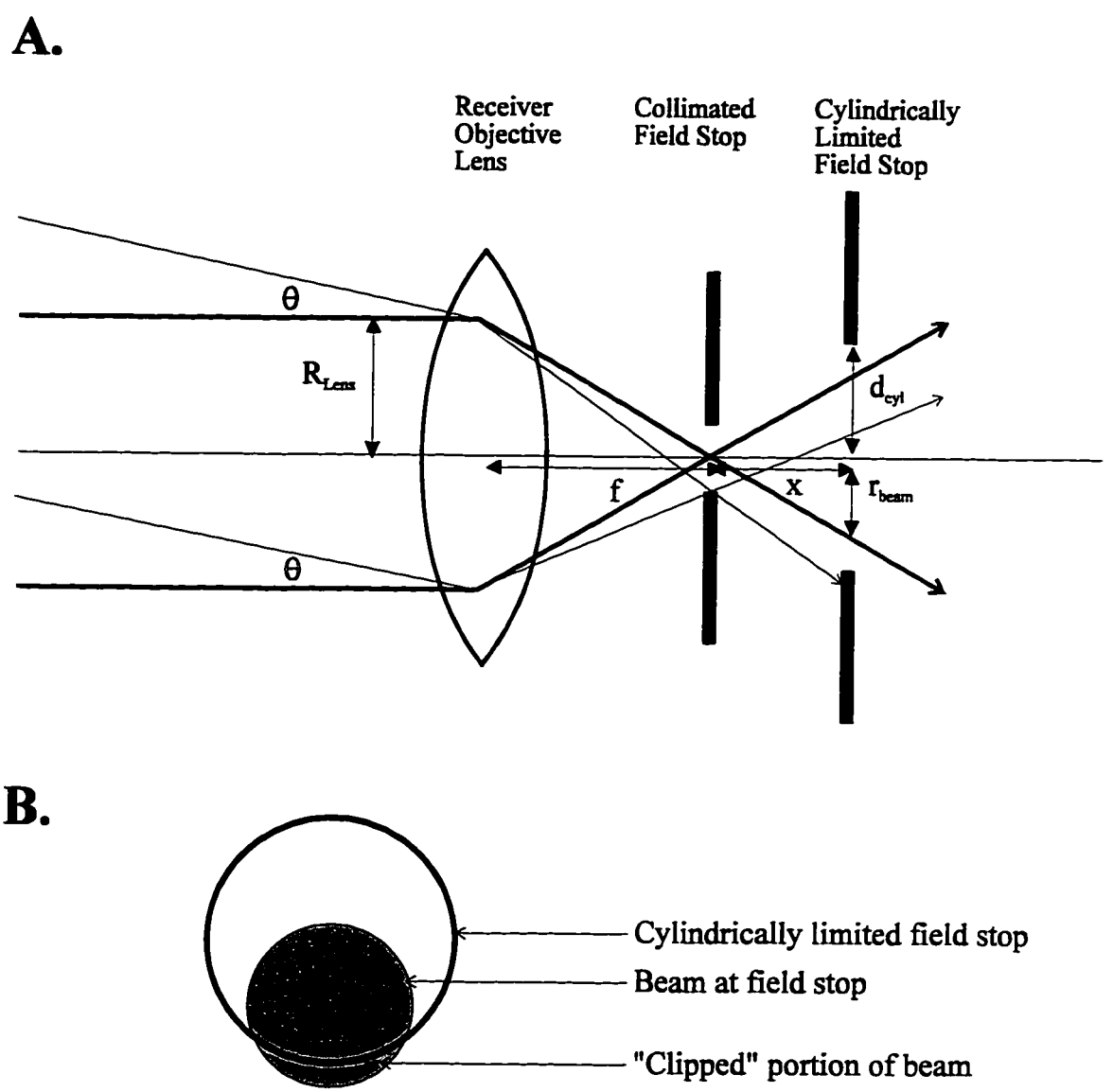

Figure 11 A. Diagram showing the effect of angular deflection in the optical path on the collimated and cylindrically limited systems. The angular deflection shown is that which leads to complete clipping of the beam when a collimated system is used. The clipped portion of the beam when the cylindrically limited system is used is considerably less, and can be calculated by computing the area of the beam which lies outside of the field stop.

Figure 11 B. Axial view of the clipped beam at the field stop of the cylindrically limited system.

collimated system -- one can obtain a measure of the relative sensitivity of each system to deflection of the optical path.

In the cylindrically limited system the radius of the beam at the receiver field stop is:

$$r_{beam} = x\sin[\tan^{-1}(\frac{R_{lens}}{f})]$$

where R_{lens} is the radius of the receiver objective lens and x is the distance between the field stop and the focal plane of the lens. This reduces to

$$r_{beam} = \frac{xR_{lens}}{f} \qquad (8)$$

when f is large compared to R_{lens}. If the receiver field stop for the cylindrically limited system is built with the same amount of clearance around the beam as the collimated system, then the radius of the cylindrically limited field stop will be

$$d_{cyl} = \frac{xR_{lens}}{f} + d_{col} \qquad (9)$$

The center of the beam in the plane of the field stop and the center of the field stop will be a separated by a distance:

$$d_{err} = \theta(x+f) \qquad (10)$$

Given the radius of the field stop, the radius of the beam at the field stop, as well as the distance between their centers, it remains to find the area of the beam which lies outside the field stop. It is this area which will be clipped and lead to an error in transmittance.

Given a larger circle of radius R and a smaller circle of radius r separated by a distance d, the area of the smaller circle outside the larger can be expressed as:

$$A = 2da + [a\sqrt{r^2-a^2} + r^2\sin^{-1}(\frac{a}{r})] - [a\sqrt{R^2-a^2} + R^2\sin^{-1}(\frac{a}{R})] \quad (11)$$

where a is defined as

$$a \equiv \sqrt{r^2-[\frac{R^2-d^2-r^2}{2d}]^2}$$

when d $\langle$ r. Substituting r_{beam} (equation 8) for r, d_{cyl} (equation 9) for R, and d_{err} (equation 10) for d, equation 11 can be solved for the area of the beam which is clipped by the field stop.

For values typical of the Martek XMS transmissometer (f = 100 mm, R_{lens} = 10 mm, and x = 10 mm), the area of the beam which is clipped is 1.4 % of the area of the beam at the field stop. The collimated beam system would have an error of 100 % for the same angular deflection. This implies that the cylindrically limited system is on the order of 70 times more forgiving of mechanical instability than the collimated system.

The original Martek transmissometer optics feature a cylindrically limited optical system. A prototype collimated beam system was developed which uses the same optical

path. The collimated system showed a large (>50%) reduction in signal when the optical path was subject to 50 decibars of pressure, both in water and in an air-filled pressure vessel. No reduction in signal was observed when the cylindrically limiting optics were used and the same pressure was applied. Finger pressure on the porro prism which turns the Martek transmissometer beam back on itself shows that its mounting is not entirely rigid. We hypothesize that the reduction in signal of the collimated system was caused by clipping of the beam at the receiver field stop; the cylindrically limited system is apparently tolerant of the same degree of angular deflection. Because the porro prism is aligned and permanently potted into place by the manufacturer, we decided not to risk damaging the prism in an attempt to repair its mounting and instead used the proven Martek optics.

Forward Scattering Correction

It is a limitation of the measurement of beam attenuation that it is impossible to distinguish between photons which have been forward scattered into the field of view of the detector and those which have passed undisturbed through the entire optical path. Using an AC modulated source and synchronous detectors eliminates any error caused by ambient photons which have been scattered into the field of view of the detector, and thus minimizes the forward scattering error. Forward scattered photons from the modulated LED will still be detected, however, leading to an underestimation of the beam

attenuation coefficient.

For the collimated optical system the magnitude of the error Δc can be estimated by integrating the volume scattering function in absolute units ($sr^{-1}m^{-1}$) from 0 to the angular acceptance of the detector. For a transmissometer using collimated beam optics:

$$\Delta c = 2\pi \int_0^{\gamma} \beta(\theta) \sin(\theta)\, d\theta \qquad (12)$$

where γ is the half-angular field of view of the detector and $\beta(\theta)$ is the volume scattering function. For a collimated optical system the half-angle field of view of the detector is given by equation 7. The field of view is reduced in water according to Snell's law by the ratio of the indices of refraction of air (1.000) and water (1.340), or about 75%.

The volume scattering function in the near forward region ($\theta << \pi/2$) was described by Abramowitz and Stegun (1964) in terms of the first order Bessel function J_1:

$$\beta(\theta) = \left[\frac{x^2 J_1^2}{\theta^2} + \frac{4\mu^2 x^2}{(4\mu^2+\theta^2)^2}\right] \lambda^2/(4\pi^2) \qquad (13)$$

where m is the relative index of refraction of the scattering particle and the surrounding media and μ is m - 1. Substitution of equation 12 into equation 11 allows the integration to be performed. For the Sea Tech transmissometer, which uses a collimated system with an angular acceptance of 1 degree, the error in c is 0.01 m^{-1} at 670 nm for water with beam attenuation on the order of 0.5 m^{-1}; it increases to 0.15 m^{-1} for water with

beam attenuation coefficient on the order of 1.0 m^{-1} (Voss and Austin, 1993).

The forward scattering correction for the cylindrically limited system is more complicated than that for the collimated system because all of the light rays in the cylindrically limited system are not parallel and so the effective acceptance angle of the detector changes depending on the position and orientation of the light ray in the optical path. Voss and Austin (1993) modified the analytical correction first developed by Preisendorfer (1958) and used a semi-analytical model and Monte Carlo simulations to compare the errors due to forward scattering for the collimated and cylindrically limited systems.

Their results show that the cylindrically limited optics used in the Martek transmissometer have an error equivalent to that of a collimated beam transmissometer with an angular acceptance of 0.4 degrees. Forward scattering errors for the cylindrically limited optics were about half of those calculated for the Sea Tech optics, for five wavelength bands from 440 to 670 nm, and over beam attenuation coefficients ranging from that of pure water to over 1.0 m^{-1}. At 440 nm they predict errors of 0.01 m^{-1} in waters with attenuation coefficient 0.1 m^{-1} and errors of 0.04 m^{-1} in waters with attenuation coefficient 0.5 m^{-1} .

Transmissometer Precision

Austin (1977) analyzes the precision of a beam transmissometer along these lines:

From equation 1,

$$T_z = e^{-cz} \tag{14}$$

where T_z is defined as I(z)/I(0), c is the total beam attenuation of the water being measured at the wavelength at which the transmissometer projects, and z is the path length of the instrument. It follows that:

$$c = \left(\frac{-1}{z}\right) \ln(T_z)$$

Differentiating both sides with respect to T yields:

$$\frac{dc}{dT} = -\frac{1}{(zT_z)}$$

The fractional error in c is dc/c; dividing both sides by c we obtain:

$$\frac{dc}{c} = \left(\frac{1}{c}\right)\left(\frac{1}{z}\right)\left(\frac{-dT}{T}\right)$$

where dT is the electronic precision associated with the instrument. Replacing T by e^{-cz} we conclude that:

$$\frac{dc}{c} = \frac{(dT)\, e^{cz}}{cz} \tag{15}$$

The precision of a transmissometer is a function of its path length z, the electronic

precision dT, and the beam attenuation coefficient *c*. The path length and electronic error are typically fixed parameters for a given instrument. The beam attenuation coefficient is dependent not only on wavelength but also on the properties of the water being measured. Some knowledge of the expected concentrations of chlorophyll, particles, and dissolved organic matter is therefore necessary to design a precise transmissometer. A transmissometer that gives precise results in turbid harbor water will not give equally good results in clear open ocean water, and vice versa. Figure 12 shows the percent error in beam attenuation coefficient for the total attenuation spectra of figures 5 through 7 as measured by a transmissometer with a 1 meter path length and electronic error of 0.1%.

The error in total attenuation is larger in the blue region of the spectrum than in the red for all but the most turbid water (figure 12). The error in total attenuation is calculated from the total attenuation coefficient. The attenuation which is of interest in this application is the attenuation due to particles. This leads us to calculate the error in attenuation due to particles alone. The error in particle attenuation is always larger in the red region of the spectrum than in the blue (figure 13). The error in the particle attenuation is about 10% at 450 nm and 15% at 660 nm for a typical oligotrophic chlorophyll concentration of 0.1 mg m^{-3}.

Equation 15 can be differentiated with respect to path length z. By setting the derivative to zero and solving for z we can calculate that the resulting minimum for percent error occurs when $z = 1/c$. For a chlorophyll concentration of 0.1 mg m^{-3} the

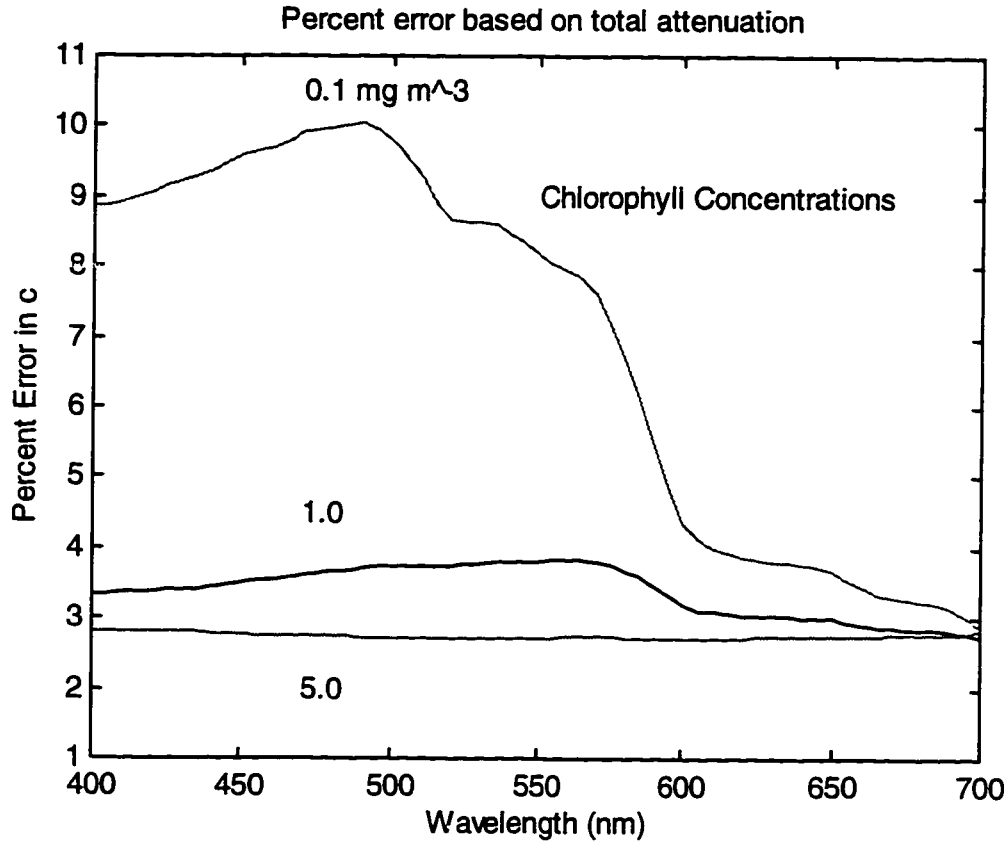

Figure 12. The precision in the measurement of beam attenuation for the total attenuation spectra of figures 5 through 7 as measured by a transmissometer with a 1 meter pathlength and electronic error of 0.1%.

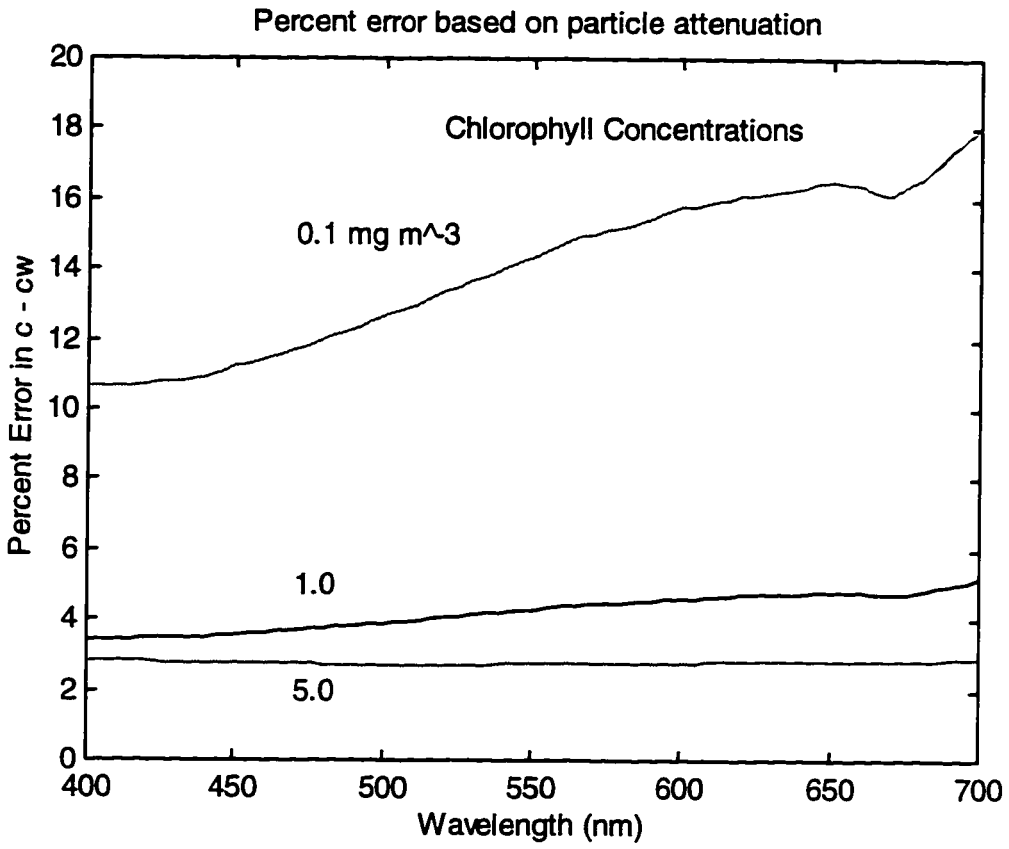

Figure 13. The precision in the measurement of beam attenuation due to particles alone. Attenuation due to particles is the total attenuation minus that of pure water.

model of Morel (1988) predicts an attenuation coefficient at 450 nm of 0.125 m^{-1} and an attenuation coefficient at 660 nm of 0.471 m^{-1}. These correspond to optimum path lengths of 8.0 and 2.1 meters. Instruments with such long path lengths are not practical for mobile field deployment; some compromise is necessary in the consideration of this design parameter. Folded paths using either prisms or mirrors can reduce overall instrument size but at the expense of some increase in optical complexity and cost.

Accuracy

The accuracy of a transmissometer depends to a large degree upon its calibration. The discussion of transmissometer calibration methods again follows that of Austin and Petzold (1977). Calibrating a beam transmissometer in pure water seems to be the most straightforward calibration method but is largely precluded by the practical difficulties of obtaining pure water and introducing the instrument to a test tank without contaminating the water. Smith and Baker (1981) calculated the attenuation of pure water at 450 nm to be 0.0190 m^{-1}. Tests with diatomaceous earth show that 1 mg/liter of suspended material corresponds to a beam attenuation coefficient of about 1 m^{-1} (Sea Tech Inc., 1994), so 0.01 mg/liter of contamination will lead to an error on the order of 0.01 m^{-1}, or 50%. For the 15 liter test tank required to completely submerge the optical path of the instrument used here, 0.15 mg of contamination will cause an error on the order of 50%, assuming the contaminating particles are optically similar to diatomaceous earth.

Calibrating a beam transmissometer in air is a more practical calibration method and can be performed accurately with some effort under most shipboard conditions. The end windows must be carefully cleaned, first with a high quality solvent (i.e. HPLC grade acetone) and then with deionized water until the output of the instrument is maximized. One must account for the difference in Fresnel reflectance when the instrument is in air and in water. At normal incidence, Fresnel reflectance of a beam of light travelling from material of one index of refraction to another is given by:

$$R = \frac{(n_1 - n_2)^2}{(n_1 + n_2)^2} \qquad (16)$$

where n_1 and n_2 are the indices of refraction of the two materials. Considering glass-to-air and glass-to-water interfaces the ratio of transmittance in air and transmittance in water can be calculated. Transmittance in air is:

$$T_a = 1 - R_a$$

while transmittance in water is given by:

$$T_w = 1 - R_w$$

where R_a is calculated from equation 15 with n_1 equal to index of refraction of air (1.000) and n_2 equal to the index of refraction of glass (1.516). R_w is calculated from equation with n_1 equal to index of refraction of water (1.340) and n_2 equal to the index of refraction of glass (1.516). The ratio T_a/T_w is equal to 0.962, at each interface. A

transmissometer such as the Sea Tech 25 cm path instrument with two interfaces will have an air calibration value of $(0.962)^2$ or 92.5% while a folded path instrument with four interfaces will have an air calibration value of $(0.962)^4$ or 85.5%. After carefully cleaning the transmissometer windows and setting the output voltage to zero with the optical path blocked, the output of a 5 Volt system is set to 5.000 x 0.855 or 4.275 Volts. The windows should be cleaned and output voltage recorded in air prior to each cast so that the effect of any drift during the course of a cruise may be corrected. In terms of output voltages, equation 1 becomes:

$$V_w = V_a \left(\frac{1}{0.855}\right) e^{-cz} \tag{17}$$

and the beam attenuation coefficient is given by:

$$c = \left(-\frac{1}{z}\right) \ln\left(\frac{0.855 V_w}{V_a}\right) \tag{18}$$

where V_w and V_a are the output voltages in water and air respectively. It is important to note that calibrating a beam transmissometer in air is only valid if the instrument is properly aligned -- all the light that reaches the signal detector in air must reach the detector in water, less only the fraction which is attenuated by the water and any dissolved or particulate materials therein.

Sensitivity

A frequent use of the beam transmissometer is to make inferences regarding the nature and concentration of particulate matter in the ocean. The optical properties of a particle in the ocean depend on its properties -- namely its size, shape, and index of refraction. The optical properties of a distribution of particles depend on the distribution of the physical properties of the population of particles. These properties are not constant so it must be expected that the relationships between the physical and optical properties of seawater will change from place to place. However, it may also be expected that these relationships will be fairly constant within a given oceanographic regime -- to such a degree that meaningful conclusions may be drawn about the physical state of the water within that regime from optical measurements.

The theoretical foundation for describing the attenuation of light by small particles in a liquid suspension is provided by Van de Hulst (1957) and Zaneveld *et al.* (1982), among others. Baker and Lavelle (1984) summarize the relationship between beam attenuation coefficient c and particles of diameter d and a given number concentration as follows:

$$c = K(d)\, N(d)\, \frac{\pi d^2}{4} \qquad (19)$$

where K(d) is a function which describes the efficiency of scattering and N(d) describes

the number concentration of the particles in the suspension. After Zaneveld et al. (1982) the particles are assumed to be non-absorbing. For non-absorbing particles which are large compared to the wavelength of the scattered light and whose index of refraction is close to that of water, (m-1 << 1 and x = $\pi d/\lambda$ >> 1) the scattering efficiency function K(d) is described by:

$$K(d) = 2-(\frac{4}{\sigma})\sin(\sigma)+\frac{4}{\sigma^2}(1-\cos(\sigma)) \qquad (20)$$

where λ is the wavelength in water of the transmissometer and $\sigma = 2x(m-1)$. Because some of the scattering will occur in the forward direction into the field of view of the detector, the scattering efficiency which is observed will be slightly different from the theoretical scattering efficiency which is predicted by equation 20 above. The relationship between the theoretical and observed scattering efficiency is:

$$K_{obs} = K_{theo}(1-\frac{b_f}{b})$$

where b_f is the scattering into the field of view of the detector and b is the total scattering. The ratio b_f/b is approximated by:

$$\frac{b_f}{b} \approx \frac{2}{(K_{theo})} \int_0^{\gamma} (x^2 M_1(x\theta) + \frac{4\mu^2}{(4\mu^2+\theta^2)^2})\,\theta d\theta$$

where $M_1(x\theta) \equiv J_1(x\theta)/(x\theta)$ and γ is given by equation 7. Baker and Lavelle (1984) consider equation 19 in terms of mass concentration C by substituting:

$$C = \rho N(d) \frac{\pi d^3}{6}$$

into equation 19, where ρ is the particle density, so that

$$c = 3K_{theo}(1-\frac{b_f}{b}) \frac{C}{2\rho d}$$

The theoretical slope of the regression between attenuation and particulate mass concentration is

$$\alpha = \frac{3}{2\rho d} K_{theo}(1-\frac{b_f}{b}) \qquad (21)$$

If a distribution of particles with number concentration N(d) and density distribution $\rho(d)$ is to be considered then equation 21 must be integrated from upper and lower limits of particle diameter.

In practice the detailed knowledge of particle properties required for such a theoretical calculation is rarely known, certainly not at the spatial resolution which is the goal of a profiling instrument such as a beam transmissometer. Empirical correlations between beam attenuation coefficient and total suspended material (TSM) or particulate organic carbon (POC) for particular geographic regions and oceanographic regimes can be constructed from CTD calibration data acquired via water samplers during upcasts.

Although the relationship between c and TSM is that which is more intuitive, the relationship between c and POC is generally more reliable, except in waters of extremely high turbidity. This is a result of the difficulty in measuring low concentrations of TSM -- the measurement involves the weighing of filters before and after a known volume of water is filtered and is less precise than the combustion technique used to measure POC and PON (University of Maryland, 1992).

Different particle populations in different locations will yield different relationships between the physical and optical properties of the water. Figure 14 shows the relationship between beam attenuation at 490 nanometers as measured by the MLML Martek transmissometer (before it underwent its present modifications) and particulate organic carbon in productive coastal waters, a transect across the equator at 140 W (Feinholz, 1996), the MOBY mooring site (Feinholz *et al.*, 1995a), and waters about the Hawaiian archipelago (Feinholz *et al.*, 1995b). The relationship between beam attenuation and particulate organic carbon is characterized by the slope of the best fit line through each set of data. The regression data are summarized in Table 1 below. Note that the slope of the regression calculated from data acquired in Monterey Bay varies from that calculated from the Lanai mooring data by an order of magnitude. The regressions of data collected during the MOBY L-7 and MOCE-3 cruises (figure 15) also demonstrate the effect of different particle type on the relationship between physical and optical parameters. The different slopes and offsets, as well as the increased scatter in the MOCE-3 data, may be explained by the fact that all the L-7 data were acquired near the

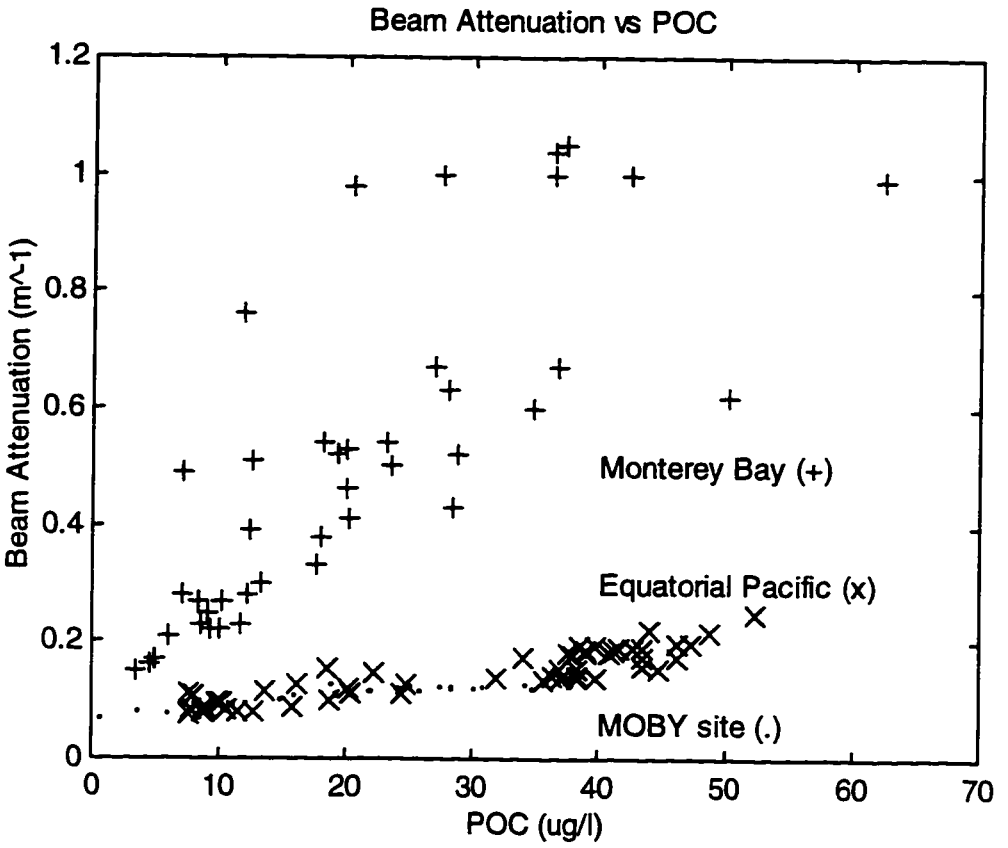

Figure 14. The relationship between beam attenuation at 490 nanometers as measured by the MLML Martek transmissometer (before it underwent its present modifications) and particulate organic carbon in productive coastal waters, along a transect across the equator at 140 W, and at the MOBY study site.

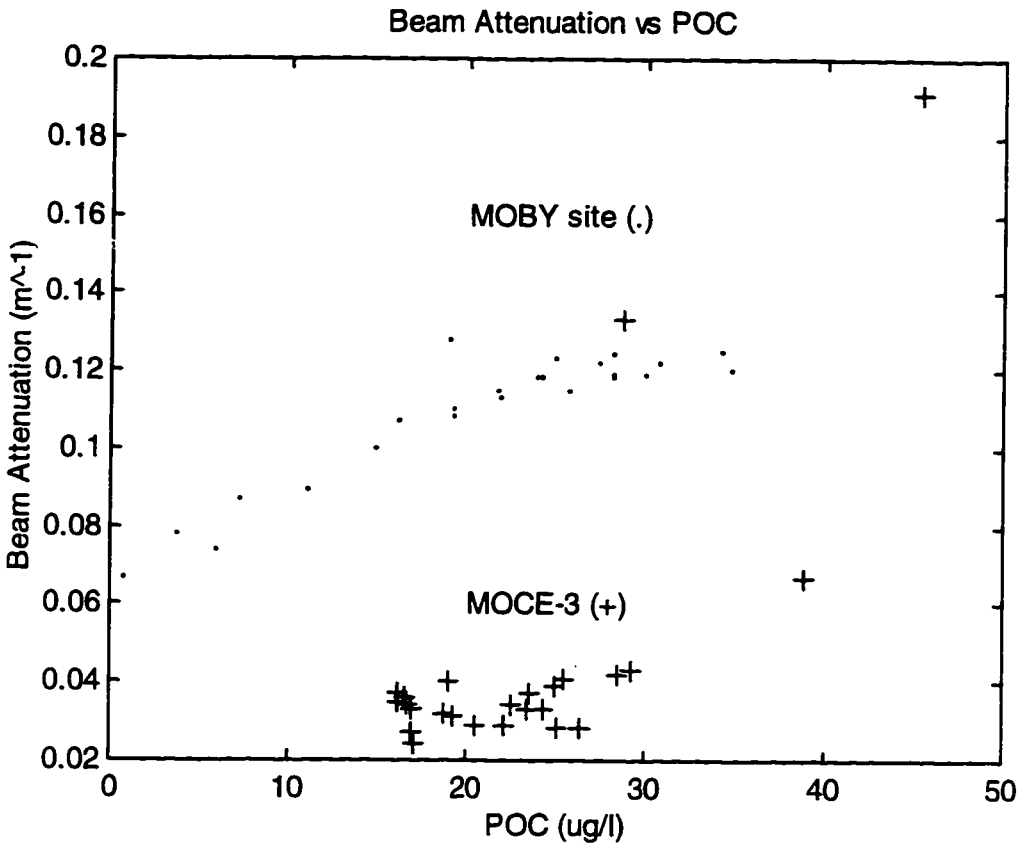

Figure 15. The relationships between beam attenuation and POC calculated from data collected at the MOBY site and during the MOCE-3 cruise about the Hawaiian archipelago.

MOBY mooring site, 10 nautical miles south of Lanai, while the MOCE-3 data were collected throughout the Hawaiian archipelago, with stations over seamounts, in regions subject to terrigenous inputs, and near harbors, as well as in oligotrophic regions. The increased scatter in the MOCE-3 data set is to be expected in light of the different particle types one expects to encounter under such widely varying conditions. The relatively good fit of the MOBY L-7 data, which is reflected in the equatorial Pacific data, is an indication of the quality of data that one can expect under homogeneous conditions.

Table 1. Summary of the relationships between particulate organic carbon (POC) and beam attenuation coefficient.

Cruise	**Location**	**Slope** $m^{-1}/(mg/m^3)$	**N**	r^2	**F**
FeLine	Equatorial Pacific	2.75×10^{-3} +/- 3.0×10^{-4}	55	0.81	225
MOCE-1	Monterey Bay	1.62×10^{-2} +/- 4.0×10^{-3}	43	0.61	65.1
MOBY L-7	Lanai Mooring	1.66×10^{-3} +/- 3.1×10^{-4}	25	0.84	121
MOCE-3	Hawaiian Archipelago	3.81×10^{-3} +/- 1.5×10^{-3}	25	0.55	27.8

Methods

The optics and electronics of a Martek XMS transmissometer were modified and the sytem's performance was assessed via an array of laboratory and field tests. The optics were modified to use a light emitting diode as the light source. An LED was selected as the source to replace the incandescent bulb of the original Martek design. New AC electronics (figure 16) were designed by Dr. Sarma Lakkaraju of the San Jose State University Physics Department. Table 2 summarizes the different design features of the original Martek, modified Martek, and Sea Tech transmissometers.

Table 2. Summary of the design features of the Martek, modified Martek, and Sea Tech transmissometers.

Instrument	Martek XMS	Modified Martek	Sea Tech
Optics	Cylindrically Limited	Cylindrically Limited	Collimated Beam
Path Length	1 meter	1 meter	25 cm
Electronics	DC	AC	AC
Source	1 Watt bulb	blue LED	red LED
Source Stability	feedback via second detector	ratios output of 2 detectors	temperature compensated
Wavelength	490 nm	450 nm	660 nm

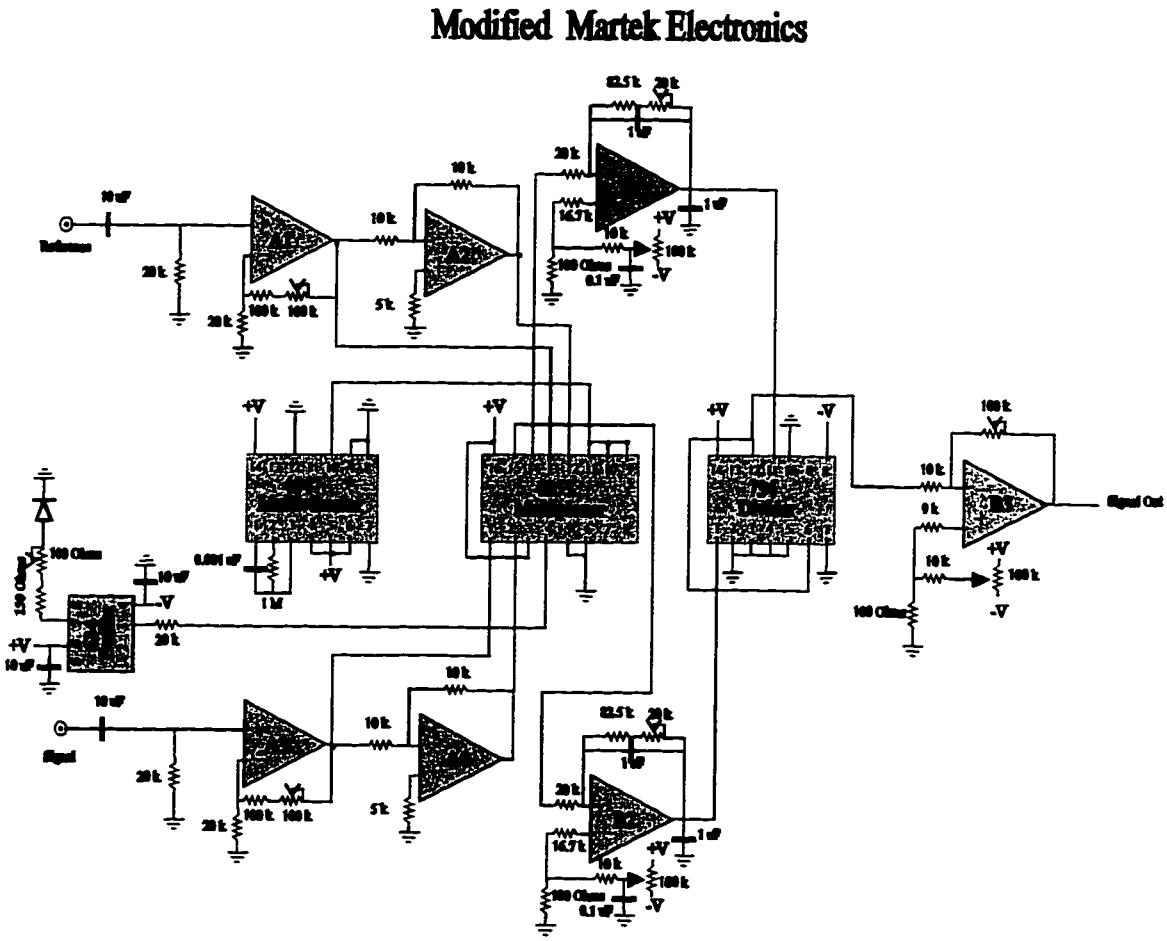

Figure 16. Modified Martek electronics by Dr. Sarma Lakkaraju of the San Jose State University Physics Department. The circuit ratios the integrated AC signals from the signal and reference photodetectors. The 4047 Multivibrator modulates the output of the LED and toggles the 4053 Multiplexer so that the integrators B1 and B2 integrate first the in-phase and then the reversed-phase signals. The circuit exhibits precision on the order of +/- 3 millivolts (0.06%).

Recent advances in LED design have led to the production of a relatively inexpensive ($8.00) high brightness blue LED which is suitable for a beam transmissometer light source. Using a solid state LED as the source eliminates the need for tungsten filament bulbs with their associated high infrared production, high current requirement, breakable filament, and filters necessary to achieve a monochromatic beam and reject infrared radiation. The modified Martek instrument uses a blue (450 nm, 70 nm half bandwidth) LED (Panasonic part # LNG901CF9) as its source.

The new Martek electronics are similar in some ways to those developed by Sea Tech. The light source of the Sea Tech transmissometer is a temperature compensated AC modulated LED that projects with a peak wavelength of 660 nm and a half bandwidth of 50 nm. The beam is detected at the end of a 25 cm path by an E.G. & G. UV100BG detector. The detector output is amplified, AC coupled to remove any DC signal caused by ambient field, then filtered and calibrated so that 0 to 5 V DC corresponds to 0 to 100% transmission in water (SeaTech Inc., 1994). The modified Martek electronics are nearly identical in concept to those of the Sea Tech, but differ in one key area. The modified Martek instrument uses two detectors -- one at each end of the optical path -- and takes the ratio of the two signals as the transmittance. The stability of the LED output is therefore less critical and careful resistor matching for temperature compensation is unnecessary.

The new transmissometer electronics were separated into two boards -- an AC board that modulates the source LED output and preamplifies the AC signals from the

two photodetectors (figures 17 and 18), and a DC board that integrates and ratios the output of the AC board (figures 19 and 20). The new Martek electronics work as follows. A 4047 monostable/astable multivibrator is set to oscillate at 200 Hz. It drives the LED in series with a 200 Ω resistor at 20 milliamps through a 634 buffer. The outputs of the two UDT-555 LN detectors are adjusted with a pair of non-inverting AC operational amplifiers to give the same output (with the optical path in air and end windows clean), and then reversed in phase with a pair of unity gain inverting amplifiers. A single OP404 quad amplifier is used for this preamplifier stage of the circuit. Both the amplified detector outputs and their corresponding reversed phase unity gain counterparts are then multiplexed through a 4053 multiplexer/demultiplexer, which is toggled by the output of the multivibrator. The AC signals from the detectors through the multiplexer are then converted to DC and adjusted in magnitude by a pair of integrators, again by an OP404 quad amplifier. The integrators alternately integrate the in-phase and unity gain reversed-phase signals from the detectors, which prevents the output of the integrators from saturating. An AD734 in divider mode is used to calculate the ratio of the signal and reference integrator outputs. The output of the divider is described by:

$$Divider\ Output = \frac{10*(Signal+Offset)}{(Reference+Offset)}$$

Trimmers on the integrators are used to adjust the signal and reference offsets to zero when the signal and reference paths are blocked. The output of the divider is adjusted

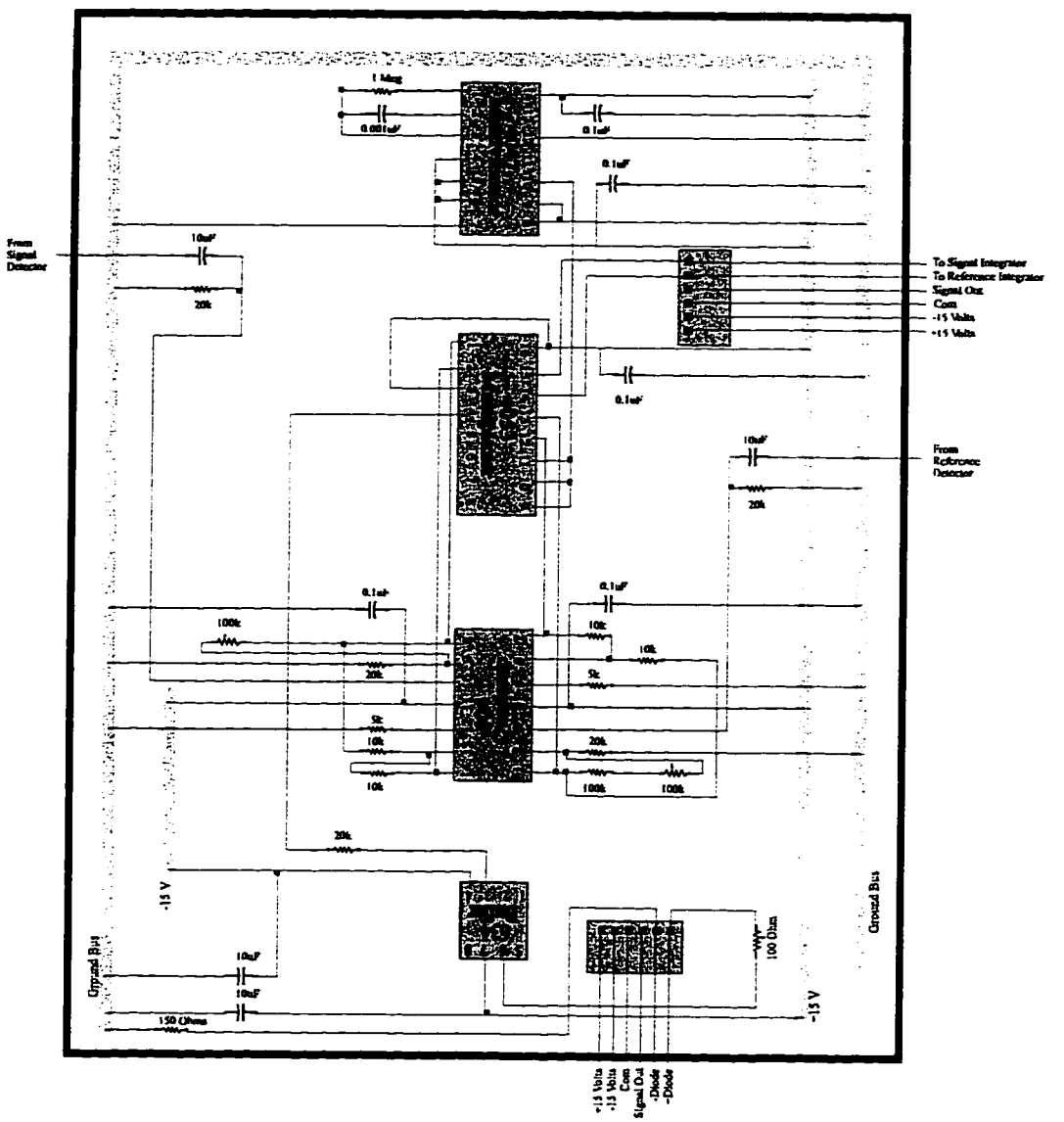

Figure 17. Layout of AC board.

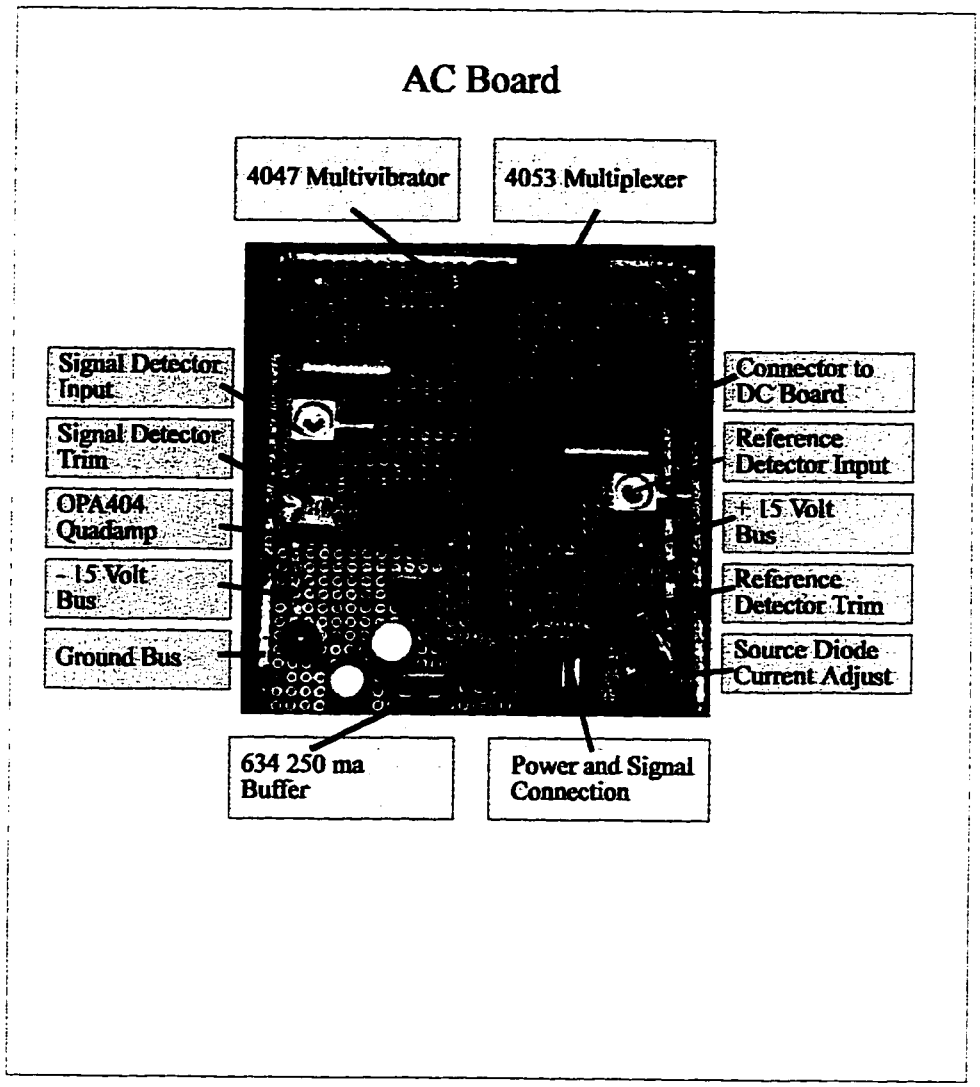

Figure 18. Photograph of modified Martek AC electronic board. Multivibrator, multiplexer, buffer, and quadamp are visible and labelled. The actual size of the board is 3.5 inches by 3.25 inches.

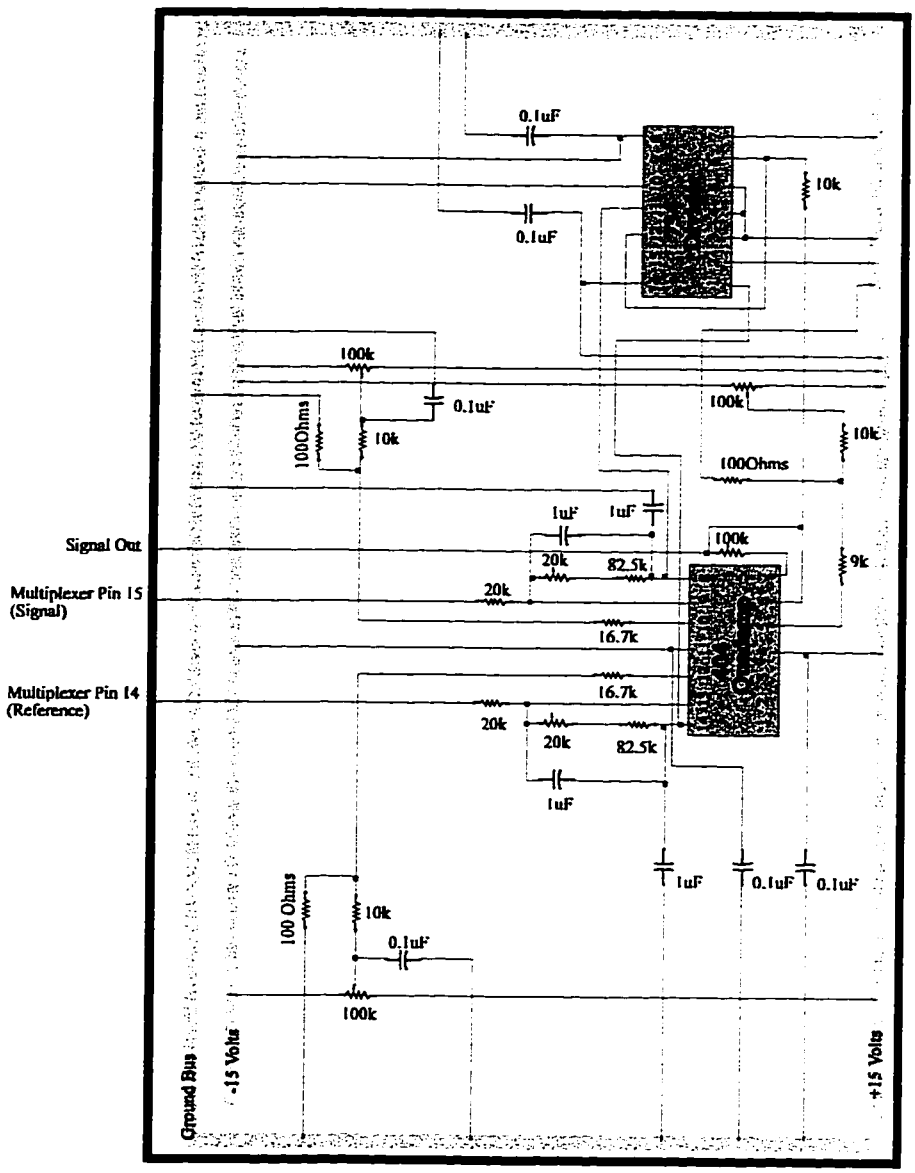

Figure 19. Layout of DC board.

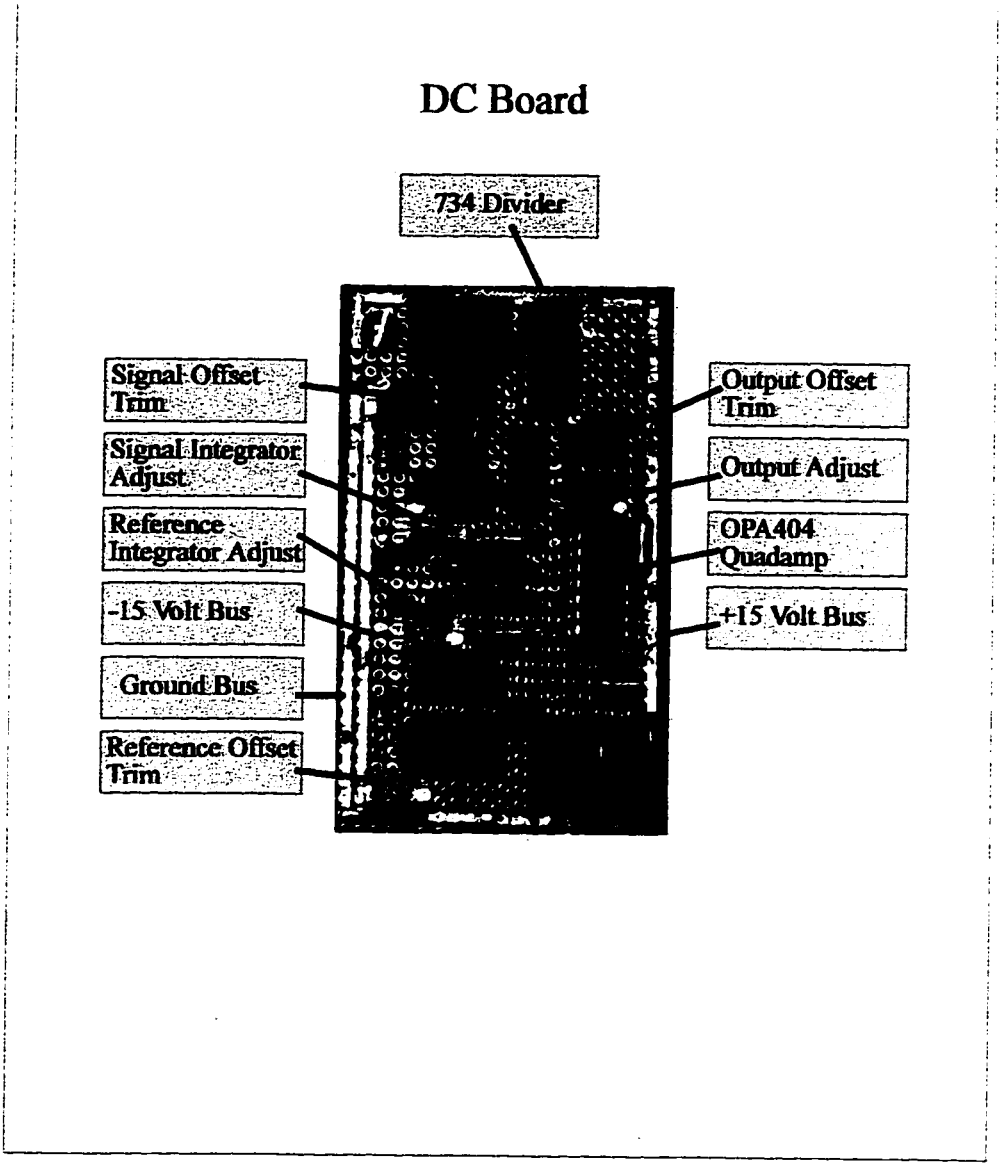

Figure 20. Photograph of modified Martek DC electronic board. Divider and Quadamp are visible and labelled. The actual size is 3.5 inches by 2.0 inches.

by the output amplifier so that 0 to 5 V DC corresponds to 0 to 100% transmission in water.

The AC amplified outputs of the detectors are insensitive to DC offsets caused by the ambient light field -- one of the advantages of an AC system. Errors caused by ambient photons scattered into the field of view of the signal detector are thus avoided, although forward-scattered photons from the LED will still be detected. A forward scattering correction may be applied to account for the latter error.

In summary, the following adjustments must be made to the circuit in order to maximize its precision:

1. Adjust the AC output of each detector so that they are equal. A multimeter in AC voltage mode should measure 0.5000 VAC at pin 7 and pin 14 of the OP404 on the AC board (figures 17 and 18). The potentiometers labelled "reference detector trim" and "signal detector trim" on figure 18 are those which must be adjusted.

2. Trim the DC output of the reference integrator so that it is zero when the power is on and the reference detector is blocked. A multimeter in DC voltage mode should measure 0.000 VDC at pin 14 of the OP404 on the DC board (figures 19 and 20). The potentiometer labelled "reference offset trim" on figure 20 is that which must be adjusted.

3. Trim the DC output of the signal integrator so that it is zero when the optical path is blocked. A multimeter in DC voltage mode should measure 0.000 VDC at pin 8 of the OP404 on the DC board (figures 19 and 20). The potentiometer labelled "signal offset trim" on figure 20 is that which must be adjusted.

4. Trim the DC output of the output amp to zero when the optical path is blocked. A multimeter in DC voltage mode should measure 0.000 VDC at pin 7 of the OP404 on the DC board (figures 19 and 20). The potentiometer labelled "output offset trim" on figure 20 is that which must be adjusted.

5. Adjust the DC output of the output amp to 4.275 Volts with the instrument in air and end windows clean. A multimeter in DC voltage mode should measure 4.275 VDC at pin 7 of the OP404 on the DC board (figures 19 and 20). The potentiometer labelled "output adjust" on figure 20 is that which must be adjusted.

Short term stability was assessed by allowing the instrument to warm up for 10 minutes and then acquiring data over 14 hours with the instrument's optical path in air. Instrument output and ambient temperature were acquired every 10 minutes by a Li-Corr LI-1000 DataLogger . Longer term drift was assessed by monitoring the output of the instrument after thorough cleaning of its end windows over 5 days, and by monitoring the air calibration value during the course of the instrument's sea trials.

The stability of the instrument with respect to ambient temperature and thermal shock was assessed by immersing its electronics in a temperature bath with its end windows clean and optical path in air. It was tested for thermal shock by rapidly immersing it in a cold (5 °C) bath while at ambient (22 °C) temperature. The temperature range in Hawaiian waters is approximately 5 to 25 °C (Feinholz *et al.* 1995b) over the upper 1000 m -- rapid immersion in the cold bath simulates the limiting case of the instrument passing rapidly through the maximum likely thermocline. Its response as a function of ambient temperature was tested by cycling the temperature bath from 5 to 22 °C, again with the optical path in air and the end windows clean and free of fog.

To test the alignment of the instrument and the linearity of its response, a turbidity test was performed in the laboratory. The instrument was calibrated in air with a red (665 nm peak wavelength, 50 nm half-bandwidth) LED used as the light source. The

instrument was then immersed in a cylindrical acrylic test tank filled with high quality (15 MΩ/cm) deionized water and the alignment adjusted so that the output was maximized. The alignment was fixed in this position. This output value was recorded, converted to an attenuation coefficient, and compared with the published values of pure water attenuation. Aliquots of diatomaceous earth were then added to the test tank which was continuously stirred by a magnetic stir bar. The optical path of the modified Martek transmissometer was immersed in the test tank and the output of the instrument was recorded for each value of total suspended material. The experiment was repeated using the blue LED as the light source.

To compare the sensitivity of the modified Martek instrument with the Sea Tech under field conditions, both instruments were integrated with the Sea-Bird 911+ CTD on the *R/V Point Sur* and mounted horizontally 25 cm apart at the bottom of a General Oceanics rosette (figure 21). Preliminary testing consisted of 4 CTD casts to 200 m in Monterey Bay during April and May 1996. To compare the accuracy of the two instruments a red LED (665 nm, 50 nm half bandwidth) was substituted for the Martek light source during one cast. Sea trials consisted of 46 casts during June and July of 1996.

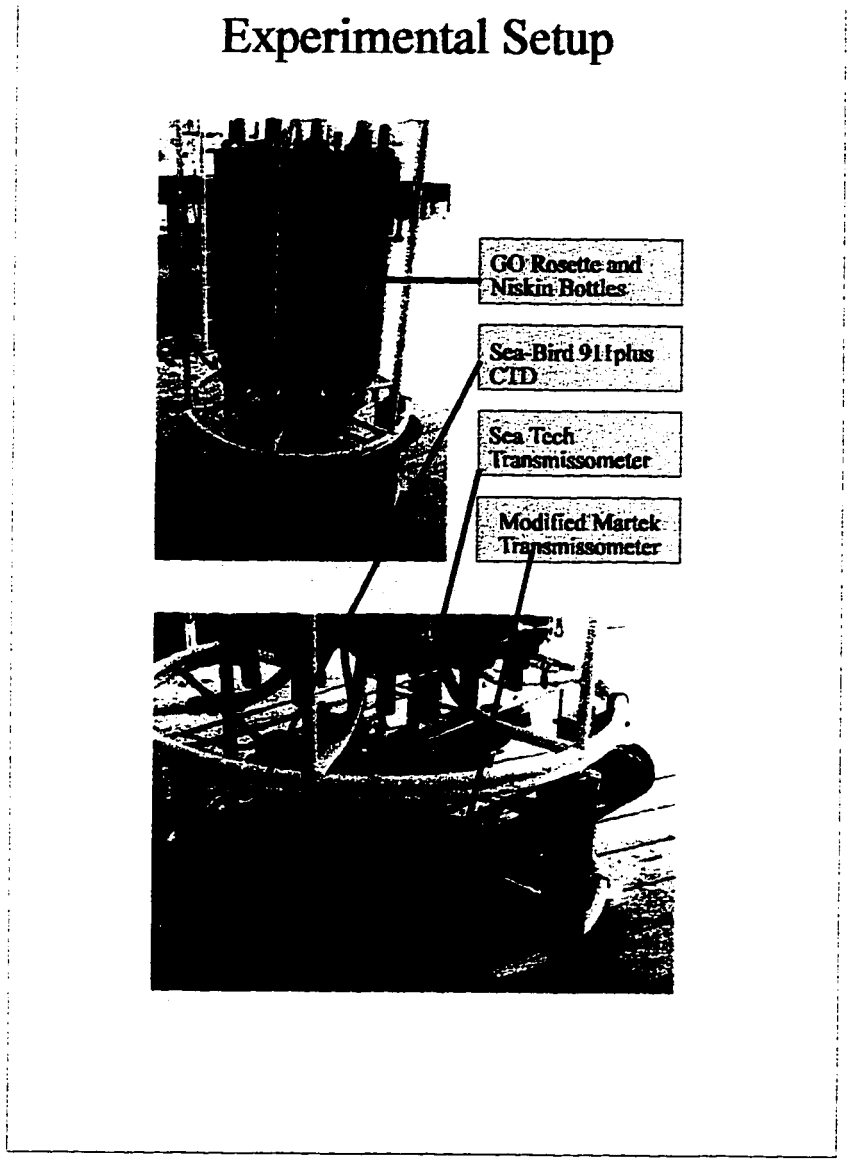

Figure 21. Experimental setup for comparison of modified Martek with Sea Tech transmissometer. Both instruments were integrated with the Sea-Bird 911plus CTD aboard the *R/V Point Sur*.

Results and Discussion

When properly adjusted the modified Martek transmissometer electronics demonstrated precision of +/- 3 millivolts during a 14 hour test period from 9 to 10 May 1996 (figure 22). This corresponds to a precision in transmission of +/- 0.06%, and absolute errors in beam attenuation of 0.0026 m^{-1} for pure water, 0.0038 m^{-1} for water with transmittance of 50%, and 0.013 m^{-1} for water with transmittance of 10%. It should be noted here that a typical 200 meter CTD cast takes about 10 minutes; a deep cast to 2000 meters takes about an hour. The errors reported here therefore represent the worst case scenario, rather than lower limits.

Longer term drift was less precisely quantified. In the laboratory, the instrument remained within the precision of its output for 5 days in August 1996. It should be noted however, that the instrument was in a temperature controlled environment (22 +/- 1°C) and the end windows remained clean for the test period. The effect of any inconsistency in cleaning the windows was therefore eliminated. The air calibrations performed by the ship's personnel during sea trials varied by 200 millivolts, but the reason for such a large discrepancy is unknown. Fog, spray, and salt can make the cleaning of transmissometer windows difficult at best while on deck at sea. In addition, residual water droplets on the windows can cause large variations in the output of the instrument. Additional experience with the new instrument under field conditions will lead to greater insight into its long

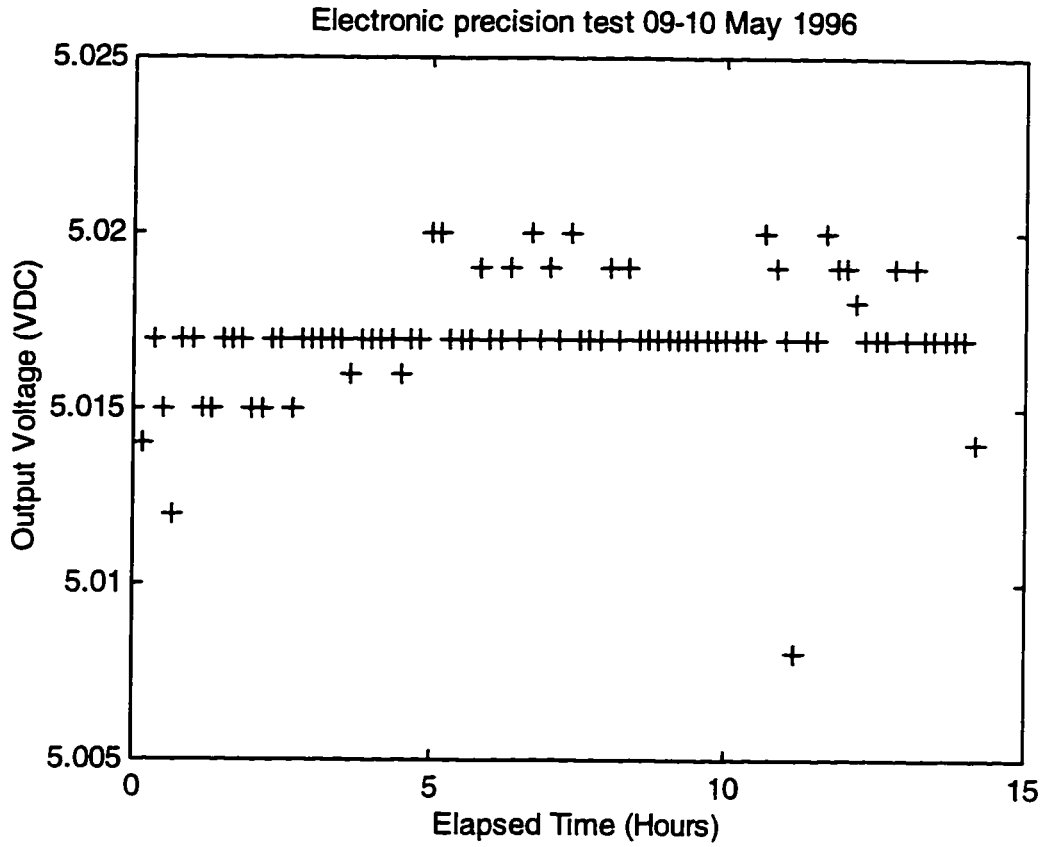

Figure 22. Voltage output of the modified Martek electronics over a 14 hour test period on 9-10 May 1996. When properly adjusted the modified Martek transmissometer electronics demonstrated precision of +/- 3 millivolts which corresponds to a precision in transmission of +/- 0.06%, and absolute errors in beam attenuation of 0.0026 m^{-1} for pure water, 0.0038 m^{-1} for water with transmittance of 50%, and 0.013 m^{-1} for water with transmittance of 10%.

term drift.

The modified Martek transmissometer is not completely immune to temperature hysteresis. For two tests of thermal shock conducted 31 May and 3 June 1996 the instrument demonstrated an effect of +/- 0.2% in transmission over a temperature range of 5 to 20 °C. This temperature range is approximately equivalent to that which is encountered over the upper 2000 meters in tropical waters. For comparison, Sea Tech cites a temperature stability of +/- 0.3% over a temperature range of 0 to 25 °C. The effect demonstrated here appears linear to first order and is equal to 2.7 +/- 0.4 millivolts/°C (N = 16, SE = 0.003 m^{-1}, r^2 = 0.926 , F = 174; $F_{0.05,1,14}$ = 4.60) (figure 23). A preliminary test indicated that the characteristic time for temperature equilibration of the electronics container with the temperature bath was on the order of 5 minutes, so data for this test were acquired every 30 minutes over the course of eight hours. Because of the magnitude of the temperature effect a temperature transducer was added to the electronics package, with the thought that a correction to the transmissometer output might be developed, similar to that by Bishop (1986) for the Sea Tech transmissometer. Such a correction may add to the accuracy of the air calibration values if the temperature is monitored at the time of the calibrations.

To compare the sensitivity to particles of the modified Martek transmissometer with that of the Sea Tech instrument, three side by side casts to 200 meters were performed on 22 April 1996 along the axis of Monterey Bay submarine canyon (figures 24 through 26). The figures show the profiles of sigma-theta and the voltage outputs of

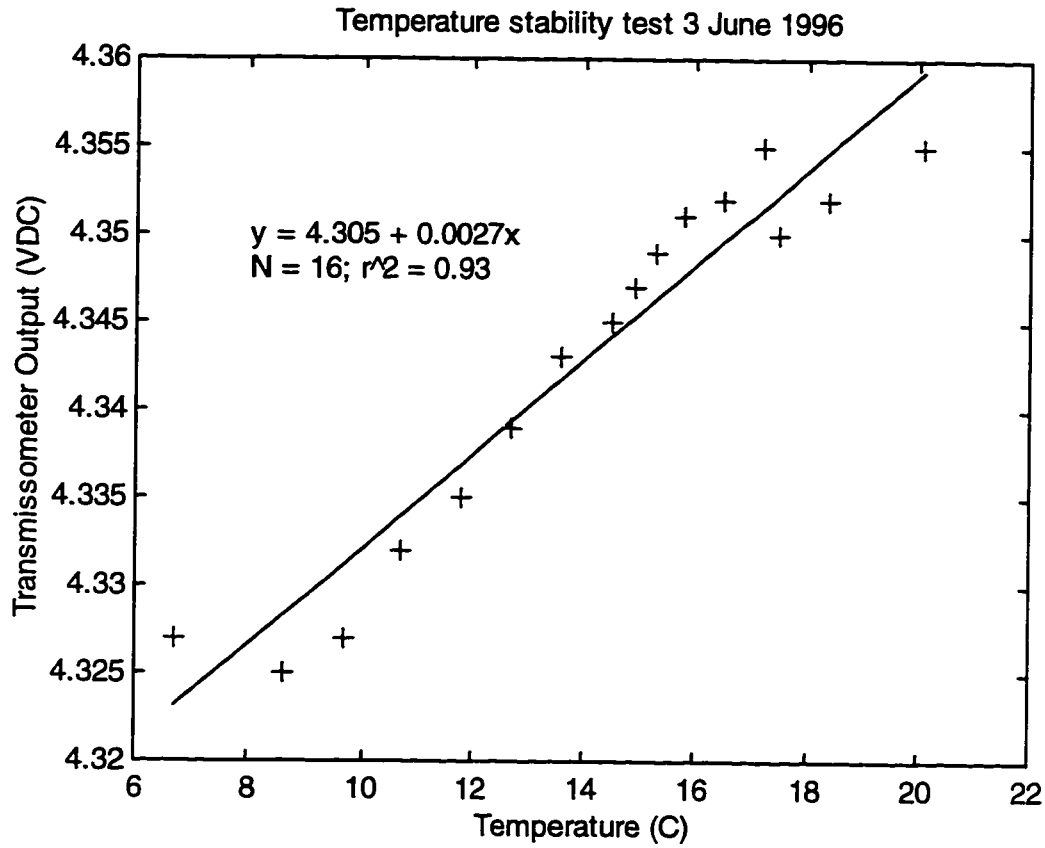

Figure 23. Output of modified Martek transmissometer plotted against the water bath temperature in which its electronics case was immersed. Data for this test were acquired every 30 minutes over the course of eight hours, and show an effect approximately equal to 2.7 millivolts per degree C.

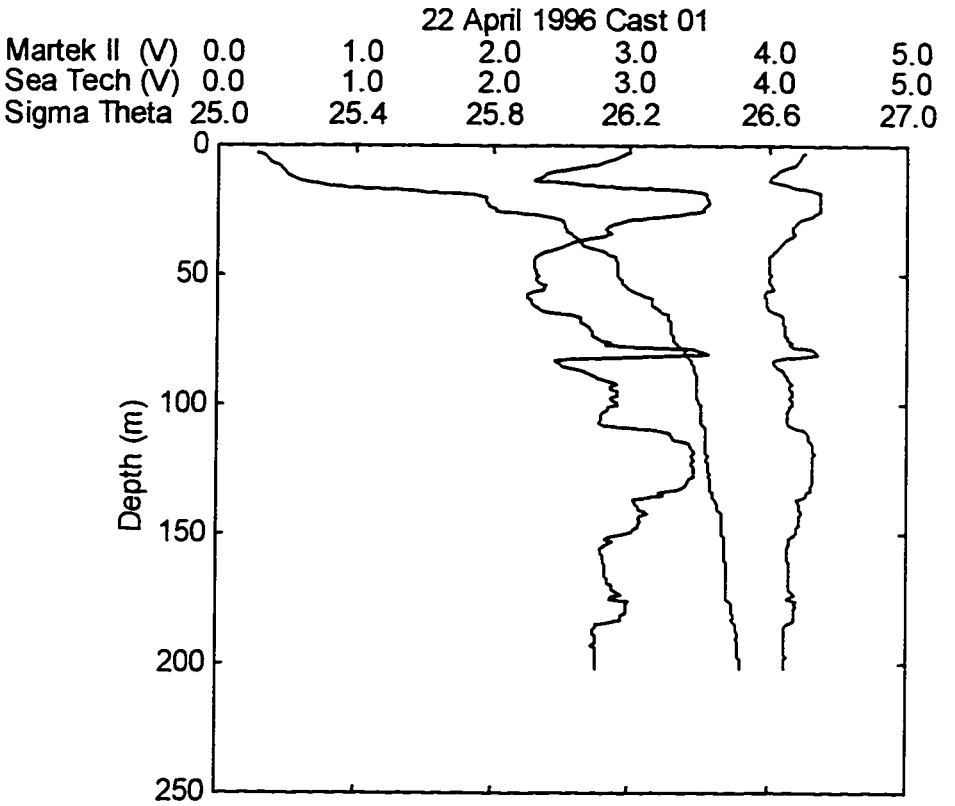

Figure 24. Profiles of sigma theta (green) and voltage outputs of Sea Tech 25 cm path (red) and modified Martek 1 m path (blue) transmissometers acquired during CTD cast 01 of 22 April 1996. Data were acquired at 36 47.7' N 121 51.2' W near the head of Monterey submarine canyon. The Sea Tech instrument uses an LED emitting at a peak wavelength of 660 nm and the modified Martek uses an LED with a peak wavelength of 450 nm.

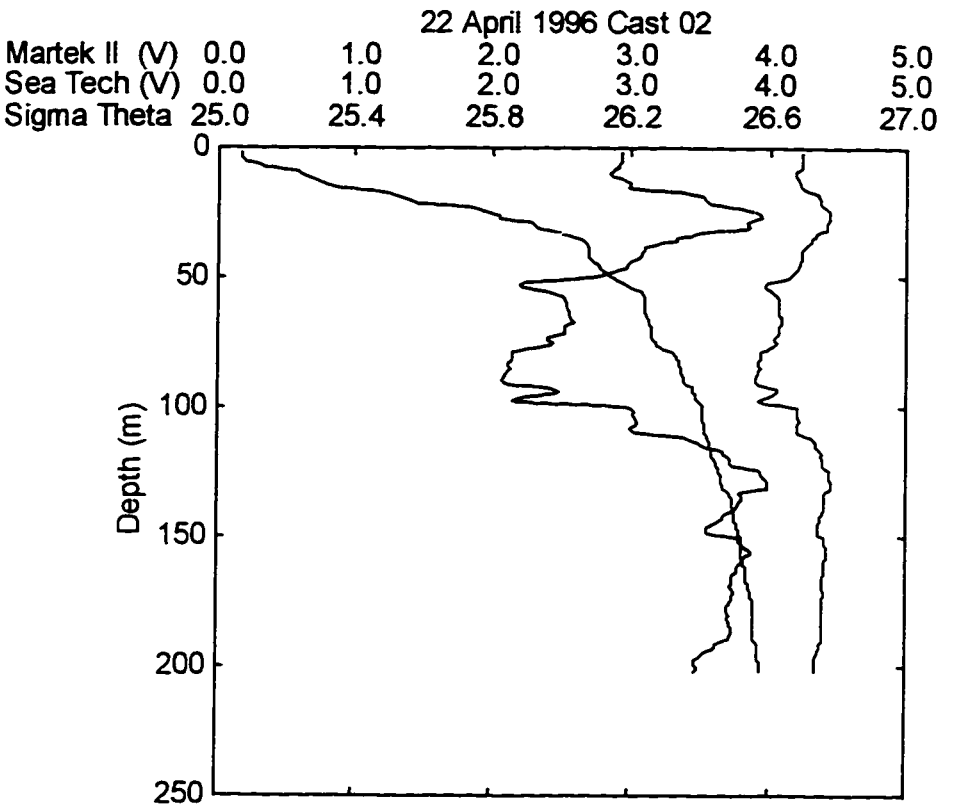

Figure 25. Profiles of sigma theta (green) and voltage outputs of Sea Tech 25 cm path (red) and modified Martek 1 m path (blue) transmissometers acquired during CTD cast 02 of 22 April 1996. Data were acquired at 36 47.2' N 121 54.4' W along the axis of Monterey submarine canyon. The Sea Tech instrument uses an LED emitting at a peak wavelength of 660 nm and the modified Martek uses an LED with a peak wavelength of 450 nm.

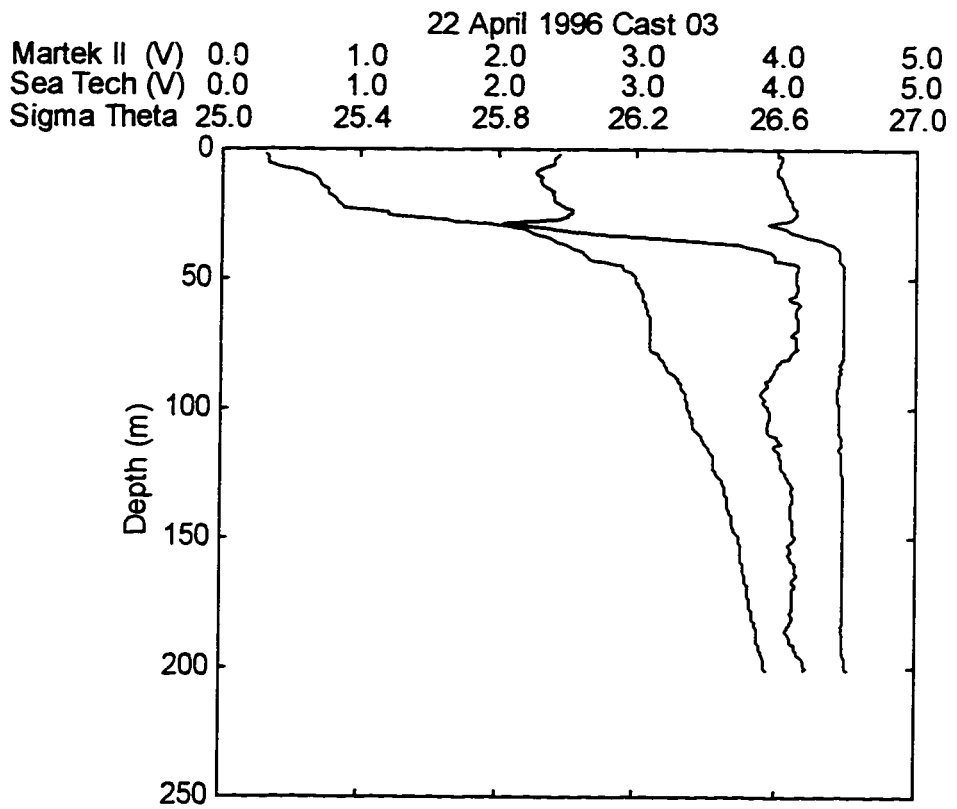

Figure 26. Profiles of sigma theta (green) and voltage outputs of Sea Tech 25 cm path (red) and modified Martek 1 m path (blue) transmissometers acquired during CTD cast 03 of 22 April 1996. Data were acquired at 36 46.0' N 121 59.5' W along the axis of Monterey submarine canyon. The Sea Tech instrument uses an LED emitting at a peak wavelength of 660 nm and the modified Martek uses an LED with a peak wavelength of 450 nm.

the two instruments after standard Sea-Bird CTD data processing (Sea-Bird Electronics, Inc., 1994). The two transmissometers track features in the water column in a remarkably similar fashion, with the increased sensitivity of the modified Martek instrument apparent. The smallest features discernable in the Sea Tech profiles are amplified in those of the Martek instrument; the smallest features in the Martek profiles are not defined in those of the Sea Tech.

The slope of the best fit line through the output of the two instruments plotted against each other (figure 27) is 3.73 +/- 0.03 (r^2 = 0.989, SE = 0.067 Volts, N = 599, F = 5.6 x 10^4, $F_{0.05,1,500}$ = 3.86). In these terms, the Martek transmissometer is 3.7 times more sensitive than the Sea Tech instrument. When the voltages were converted to beam attenuation coefficients, the corresponding slope (figure 28) is 1.25 +/- 0.01 (r^2 = 0.992, SE = 0.019 m^{-1}, N = 599, F = 7.2 x 10^4, $F_{0.05,1,500}$ = 3.86). This slope compares favorably to that predicted by the absorption and scattering models of figures 2 and 3. The absorption model of Morel (1991), and the scattering model of Gordon and Morel (1983) combine to predict a slope of 1.57. When the exponent which quantifies the wavelength dependence of scattering is set to -0.5 rather than -1.0 (after Voss (1992)) the slope predicted by the modified model is 1.22. The difference between the measured slope and that predicted by the models is consistent with a small contribution to total attenuation by dissolved organic material, which absorbs more strongly in the blue than in the red end of the spectrum. Voss (1992) analyzed spectral beam attenuation data collected over a broad geographic area and found that the slope of the regression of c_{490}

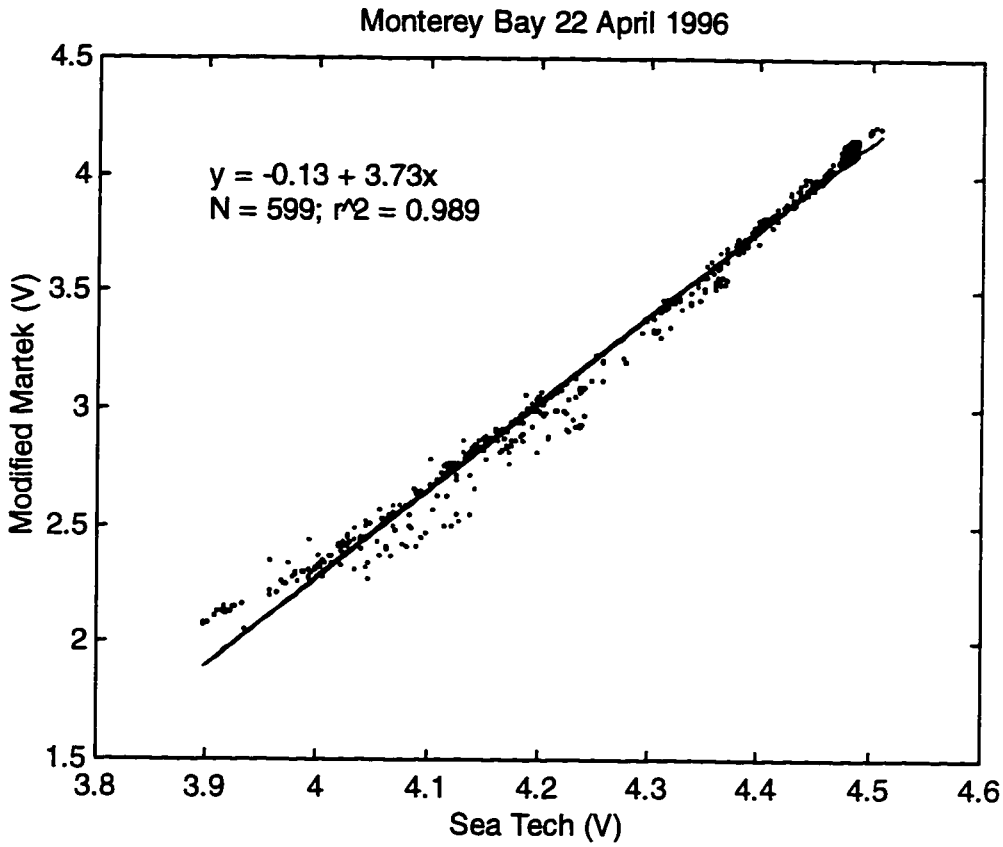

Figure 27. The output of the modified Martek transmissometer plotted against that of the Sea Tech instrument for the profiles of figures 23 through 25. The slope of the best fit line through the output of the two instruments is 3.73 (r^2 = 0.989, N = 599, F = 5.6 x 10^4, $F_{0.05,1,500}$ = 3.86). In these terms, the Martek transmissometer is 3.7 times more sensitive than the Sea Tech instrument.

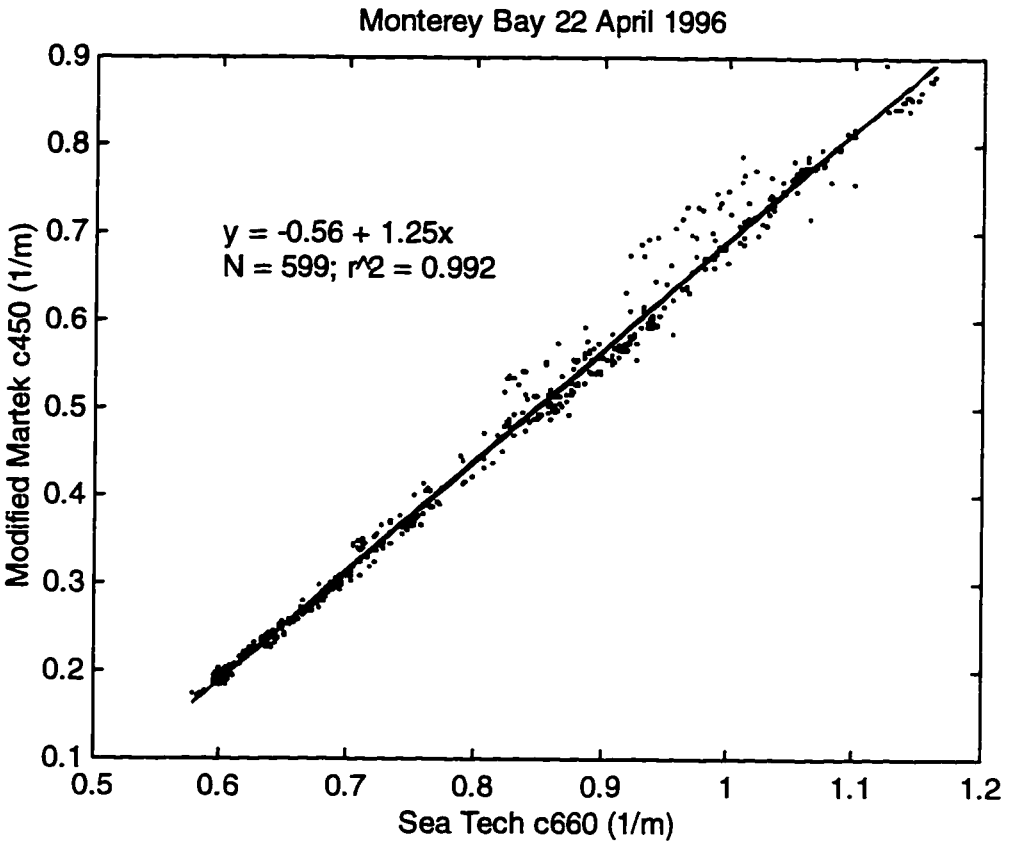

Figure 28. Beam attenuation derived from the output of the modified Martek transmissometer plotted against beam attenuation derived from Sea Tech output for the profiles of figures 24 through 26. The slope of the best fit line through the data is 1.25 (r^2 = 0.992, N = 599, F = 7.2 x 10^4, $F_{0.05,1.500}$ = 3.86).

versus c_{670} was 1.18, in surprisingly good agreement with the considerably more geographically limited set of data acquired during the course of this study, especially given the fact that the wavelength bands of the transmissometers studied by Voss (1992) are not identical with those used here.

To compare the accuracy of the modified Martek instrument with that of the Sea Tech, and to separate any effect of instrument path length from that of beam color, a red (665 nm, 50 nm half bandwidth) LED was used as the source for the Martek instrument during one CTD cast on 14 May 1996. This particular red LED was selected because among those readily available it was the closest in color to that of the Sea Tech with adequate brightness. The profiles of beam attenuation as measured by the two transmissometers show a systematic offset of 0.121 m^{-1} (figure 29). When a correction is applied to account for this offset, the two profiles are very nearly identical. When the Sea Tech and corrected Martek attenuation coefficients are plotted against each other (figure 30) the resulting regression yields an offset of 0.0038 m^{-1} and a slope of 0.996 +/- 0.005 ($r^2 = 0.999$, SE = 0.014 m^{-1}, N = 200, F = 1.8 x 10^5, $F_{0.05,1,200} = 3.89$). The offset of the Martek and Sea Tech profiles of attenuation coefficient led us to realign the Martek transmissometer before performing laboratory "pure water" and turbidity tests. This cast not only indicated that the alignment of the instrument needed to be adjusted but also confirmed that it is the difference in source wavelength, not the difference in path length, that affects the sensitivity of the beam transmissometer, at least over the range of attenuation coefficients (0.5 $m^{-1} < c < 3.0\ m^{-1}$) encountered on this cast .

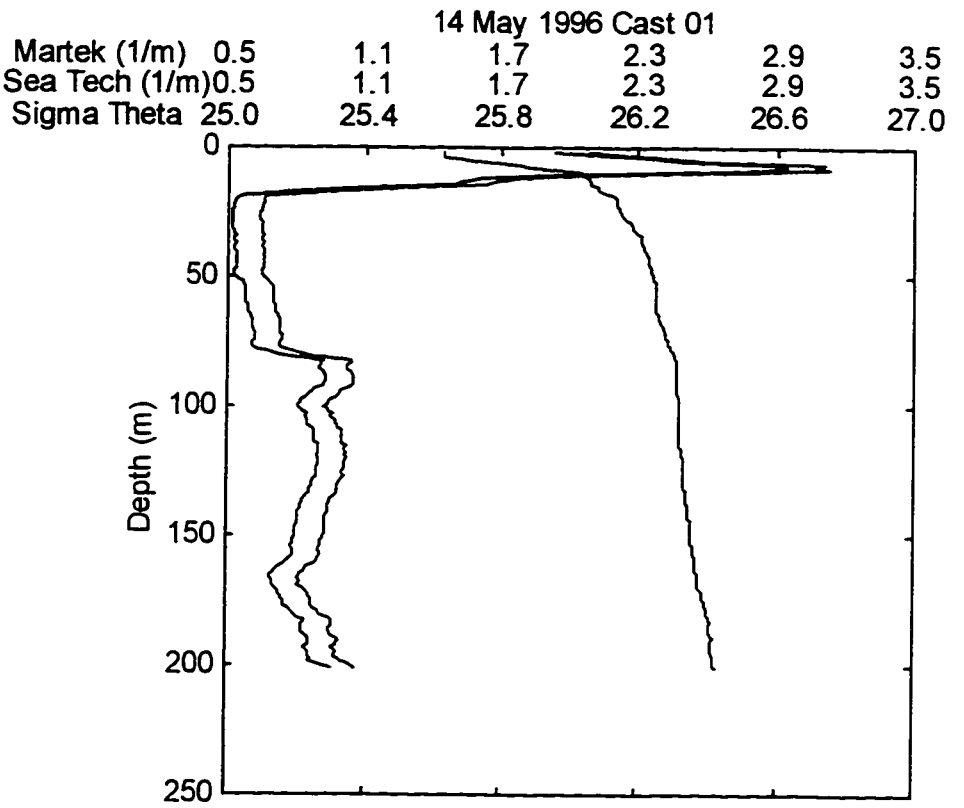

Figure 29. Profiles of sigma theta (green) and beam attenuation as measured by the Sea Tech 25 cm path (red) and modified Martek 1 m path (blue) transmissometers acquired during CTD cast 01 of 14 May 1996. Data were acquired at 36 47.7' N 121 52.2' W near the head of Monterey submarine canyon. The Sea Tech instrument uses an LED emitting at a peak wavelength of 660 nm and the modified Martek used an LED with a peak wavelength of 665 nm.

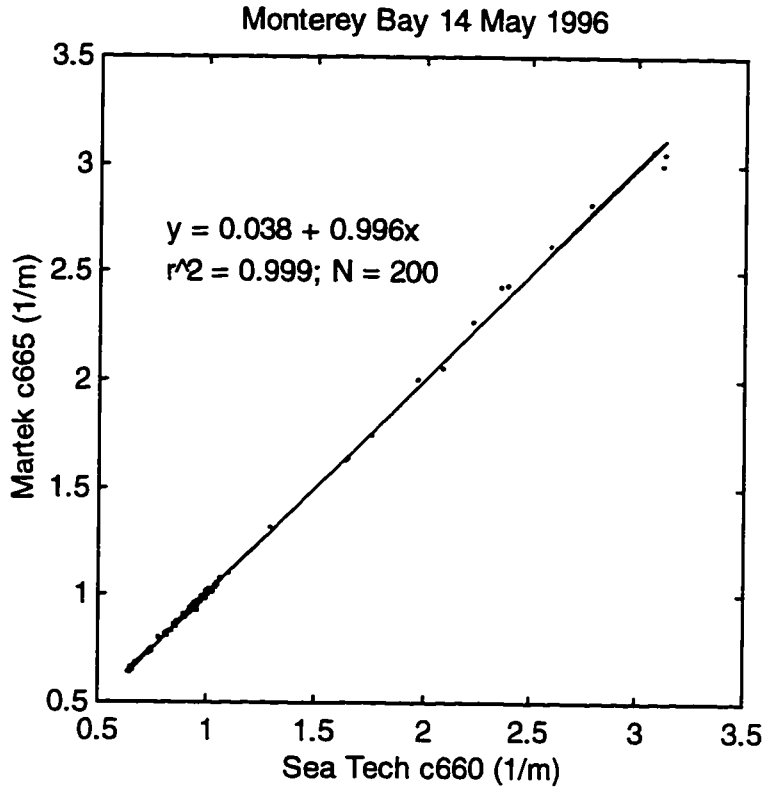

Figure 30. Beam attenuation derived from the corrected output of the modified Martek transmissometer plotted against beam attenuation derived from Sea Tech output for the profile of figure 29. The regression for the corrected data yields an offset of 0.0038 m^{-1} and a slope of 0.996 (r^2 = 0.999, N = 200, F = 1.8 x 10^5, $F_{0.05,1,200}$ = 3.89).

The "pure water" values measured at 450 and 665 nm on 6 June 1996 compare favorably with those of Smith and Baker (1981). The published value for c_{450} is 0.0190 m^{-1} and that for c_{665} is 0.4191 m^{-1}, while the values measured in the test tank were c_{450} = 0.0234 m^{-1} and c_{665} = 0.4275 m^{-1}. The measured values overestimate the published values by 0.008 m^{-1} in the red and 0.004 m^{-1} in the blue. This is consistent with the inevitable contamination of the test tank due to the introduction of the instrument into the tank. Despite careful cleaning and multiple deionized water rinses for the exterior of the transmissometer and interior of the test tank, some particles were visible following the introduction of the transmissometer. The intercepts of the turbidity regressions (c_{450} = 0.021 m^{-1} and c_{665} = 0.432 m^{-1}) also compare favorably with the pure water values of Smith and Baker (1981), although it must be noted that the standard error of the estimate in each case is 0.03 m^{-1}. The values of total suspended material in this test also exceed by two orders of magnitude those for which this instrument was designed. For these reasons, one must be wary of interpreting the intercepts of the turbidity regressions as values for pure water attenuation.

The modified Martek transmissometer demonstrated a linear response with respect to the added aliquots of diatomaceous earth (figure 31). At 665 nm the regression yielded a slope of 0.098 +/- 0.003 $(m^{-1})/(mg/l)$ (r^2 = 0.999, SE = 0.03 m^{-1}, N = 9, F = 8.8 x 10^3; $F_{0.05,1,7}$ = 5.59) while that at 450 nm was 0.099 +/- 0.002 $(m^{-1})/(mg/l)$ (r^2 = 0.999, SE = 0.03 m^{-1}, N = 9, F = 1.1 x 10^4; $F_{0.05,1,7}$ = 5.59). A similar test of the Sea Tech

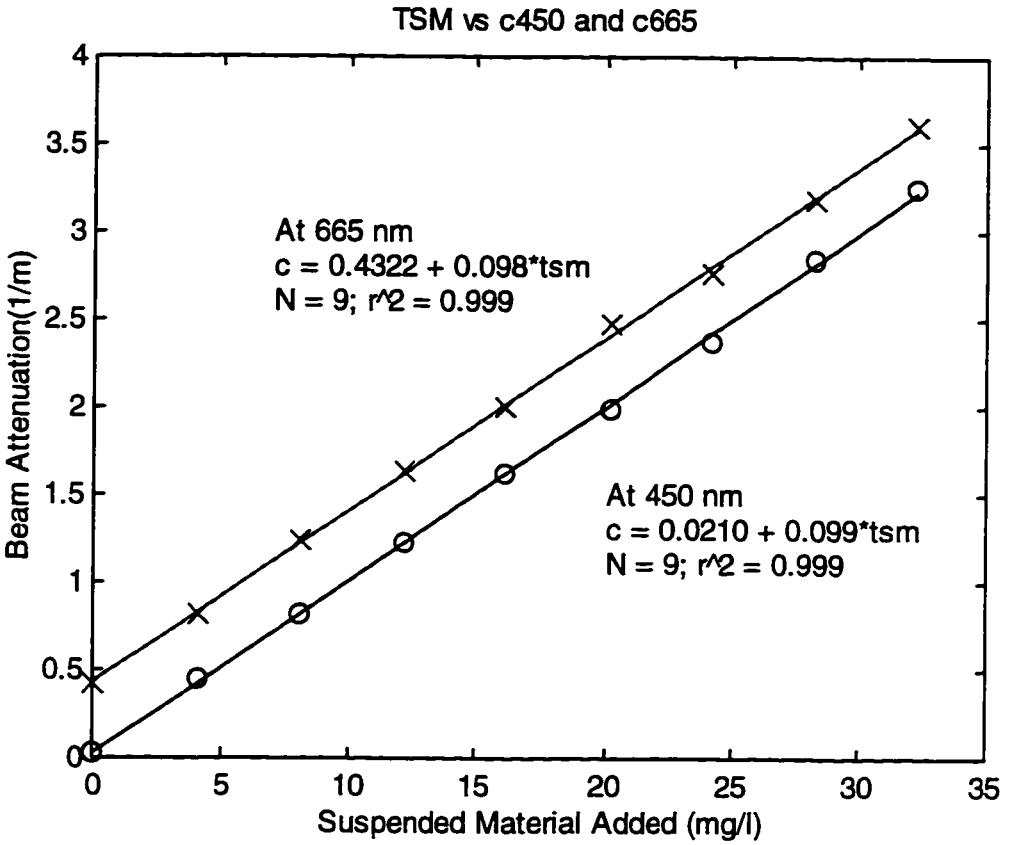

Figure 31. Beam attenuation coefficient in the red and blue from the modified Martek transmissometer plotted against the concentration of diatomaceous earth in suspension for the laboratory turbidity test of 6 June 1996. At 665 nm the regression yielded a slope of 0.098 m^{-1}/(mg/l) ($r^2 = 0.999$, N = 9, F = 8.8 x 10^3; $F_{0.05,1,7} = 5.59$) while that at 450 nm was 0.099 m^{-1}/(mg/l) ($r^2 = 0.999$, N = 9, F = 1.1 x 10^4; $F_{0.05,1,7} = 5.59$). A similar test of the Sea Tech transmissometer conducted by the manufacturer yielded a slope of 0.370 m^{-1}/(mg/l).

transmissometer conducted by the manufacturer (Sea Tech Inc., 1994) yielded a slope of 0.3701 +/- 0.0004 $(m^{-1})/(mg/l)$ ($r^2 = 1.000$, SE = 0.0018 m^{-1}, N = 11, $F = 4.0 \times 10^6$; $F_{0.05,1,7} = 5.59$).

The two slopes calculated from the modified Martek data are neither statistically nor physically different. It is somewhat disconcerting to note that the wavelength of the transmissometer source had no effect on the sensitivity of the instrument to particles. This may be explained by the fact that the scattering model of Gordon and Morel (1983) (summarized by equation 5) was empirically determined from 740 samples of natural waters collected during the course of 5 cruises from 1970 to 1979. The water sampled during the laboratory tests with added diatomaceous earth cannot be expected to have the same scattering and absorption properties as the samples from which the model was derived. The diatomaceous earth solution appears strikingly white to the naked eye -- quite unlike any of the colors that one associates with natural waters. The white appearance of the diatomaceous earth solution is consistent with the lack of wavelength dependence measured by the transmissometer during these tests.

The slope of the data published by Sea Tech Inc. (1994) differs by a factor of four from those measured here. This may be due to differences in the scattering properties of the diatomaceous earth used in the different tests, or it may be due to a difference in experimental setup. One problem in particular with our setup may be the vertical orientation of the cylindrical test tank. Despite the use of a magnetic stirrer, the solution may not have been uniform in particle concentration. Settling of the particles may have

contributed to a reduction in the effective particle concentration, and is consistent with the lower value of the slope that we measured. Redesigning the test tank and repeating the experiment may produce more comparable regressions between diatomaceous earth concentration and beam attenuation. The results of this particular test might at first glance seem to indicate that the Sea Tech transmissometer is more sensitive to particles than the modified Martek instrument but this conclusion is contradicted by tests performed under identical conditions in the field and should therefore be rejected.

The modified Martek transmissometer successfully acquired data during each of its 46 casts over the course of its sea trials during June and July 1996 off the central California coast. The increased sensitivity of the Martek instrument observed in the preliminary casts of 22 April 1996 is reflected in those of the sea trials. Again, the smallest features discernable in the Sea Tech profiles are amplified in those of the Martek instrument; the smallest features in the Martek profiles are not defined in those of the Sea Tech. Figures 32 and 33 display representative casts which illustrate the increased sensitivity of the modified Martek instrument.

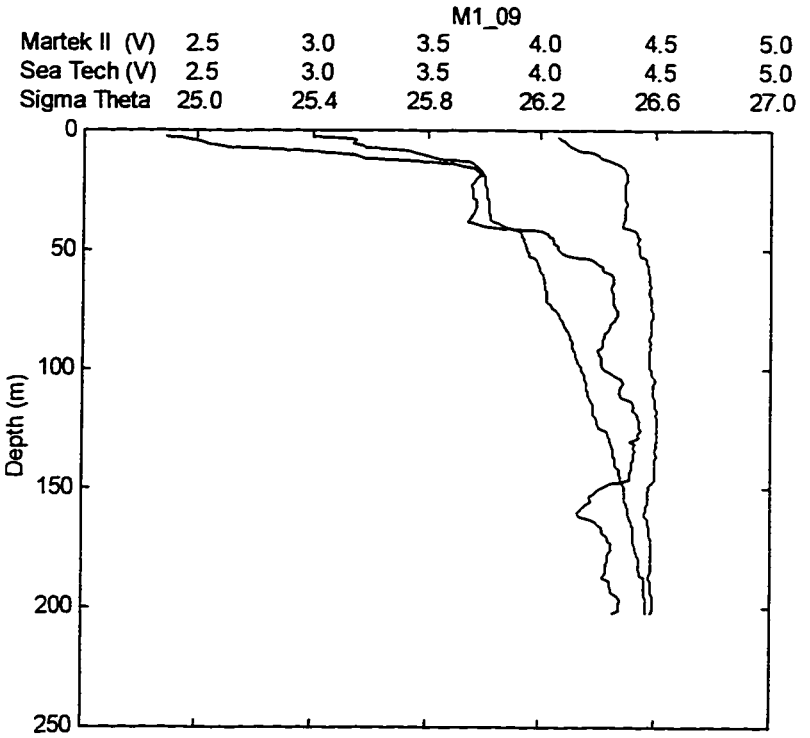

Figure 32. Profiles of sigma theta (green) and voltage outputs of Sea Tech 25 cm path (red) and modified Martek 1 m path (blue) transmissometers acquired during station M1-09 of the sea trials of the modified Martek transmissometer. Data were acquired on 02 July 1996 at 36 44.62' N 122 01.33' W in Monterey Bay. The Sea Tech instrument uses an LED emitting at a peak wavelength of 660 nm and the modified Martek uses an LED with a peak wavelength of 450 nm.

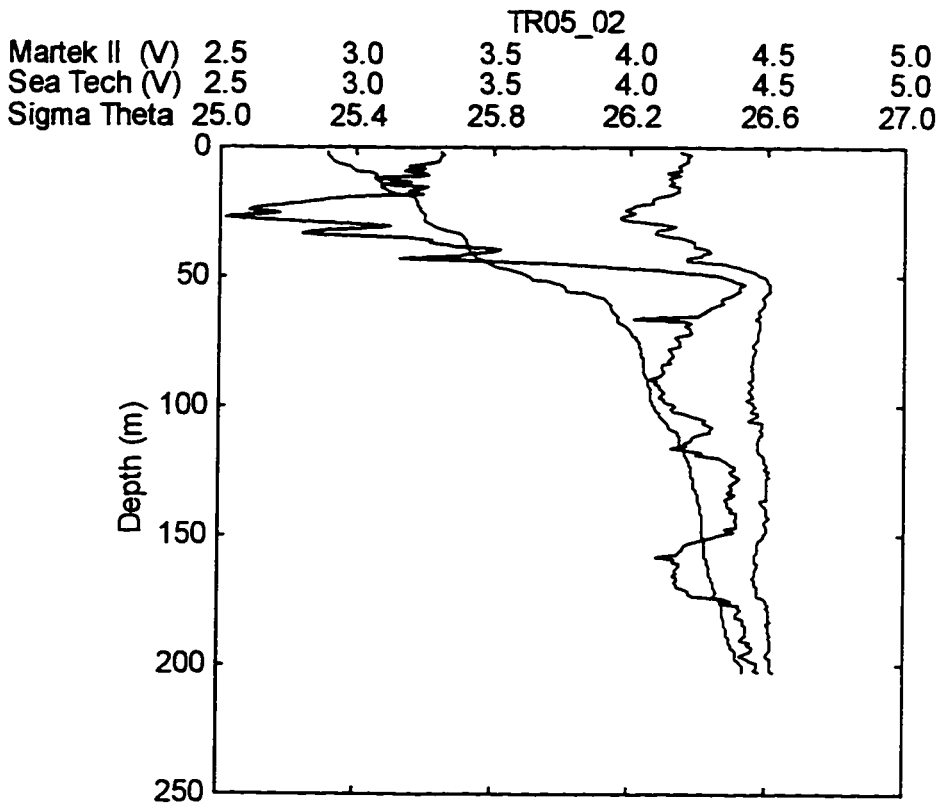

Figure 33. Profiles of sigma theta (green) and voltage outputs of Sea Tech 25 cm path (red) and modified Martek 1 m path (blue) transmissometers acquired during station TR05-02 of the sea trials of the modified Martek transmissometer. Data were acquired on 12 July 1996 at 35 28.04' N 121 21.89' W south of Monterey Bay. The Sea Tech instrument uses an LED emitting at a peak wavelength of 660 nm and the modified Martek uses an LED with a peak wavelength of 450 nm.

Conclusions

The performance of the modified Martek instrument was comparable to that of a well known commercial instrument. It demonstrated similar accuracy and stability with respect to temperature, and superior sensitivity to particles under field conditions in Monterey Bay. The increase in sensitivity to particles was due to the wavelength of the light source used, not the difference in path lengths between the two instruments. We expect the new version of the Martek transmissometer to provide the most accurate and precise profiles of beam attenuation possible during its operational deployments as part of the suite of instruments collecting data during MOBY operations.

A temperature correction algorithm may increase the accuracy of the processed transmissometer profiles. Developing such an algorithm is in principle straightforward, but further effort would be well invested in the investigation of the time dependence of the effect of temperature on the instrument's electronics. At present we have no information about whether or not this temperature effect is changing with time. Any temperature correction algorithm which is developed can be checked by comparing up-cast and down-cast profiles of beam attenuation before and after correction.

Pragmatic and geographic considerations prevented us from some comparisons which may have proved interesting, and bear further consideration. Having only one prototype instrument available, and lacking water filtering apparatus for the analysis of

particulate organic carbon in Monterey Bay, we were unable to compare the relationships between POC and beam attenuation as measured by the Martek transmissometer before and after its modifications. Cruises scheduled for the fall of 1996 in Hawaii may enable us to rectify this. The new AC electronics should provide more accurate values of beam transmission in the sunlit near surface water, and this hypothesis should be tested. This exercise could very well prove to be an interesting investigation of diurnal variations in particle properties.

It would also be interesting to compare the performance of the modified Martek and Sea Tech transmissometers in the very clear waters for which our instrument was optimized. We predict less scatter in the beam attenuation vs POC plot derived from the modified Martek data as opposed to that derived from Sea Tech data. Again, this hypothesis should be tested.

References

Abramowitz, M., and I.A. Stegun (1964) *Handbook of Mathematical Functions*, US Government Printing Office, Washington D.C. 1046 pp.

Austin, R.W. (1977) Precision considerations in the measurement of volume attenuation coefficient. In J.E. Tyler (ed.) *Light in the Sea*, Stroudsburg, Dowden Hutchinson Ross, pp. 121-124.

Austin, R.W. and T.J. Petzold. (1977) Considerations in the design and evaluation of oceanographic transmissometers. In J.E. Tyler (ed.) *Light in the Sea*, Stroudsburg, Dowden Hutchinson Ross, pp. 104-120.

Baker, E.T., and J.W. Lavelle (1984) The Effect of Particle Size on the Light Attenuation Coefficient of Natural Suspensions, *Journal of Geophysical Research*, **89**:8197-8203.

Bartz, R., J.R.V. Zaneveld, and H. Pak (1978) A transmissometer for profiling and moored observations in water, *S.P.I.E Ocean Optics V, 160*, pp.102-108.

Bishop, J.K.B. (1986) The correction and suspended matter calibration of Sea Tech transmissometer data, *Deep-Sea Research*, **33**:121-134.

Broenkow, W.W., A.J. Lewitus, M.A. Yarbrough, and R.T. Krenz (1983) Particle fluorescence and bioluminesence distributions in the eastern tropical Pacific. Nature **302**:329-331.

Broenkow, W.W., M.A. Yuen, and M.A. Yarbrough (1992) VERTEX: biological implications of total attenuation and chlorophyll and phycoerythrin fluorescence distributions along a 2000 m deep section in the Gulf of Alaska. *Deep-Sea Research*, **39**:417-437.

Broenkow, W.W., M.E. Feinholz, S.J. Flora, and J.A. Gashler (1995) Shipboard Techniques for Oceanographyic Observations. Moss Landing Marine Laboratories Technical Publication 94-2, Moss Landing, CA. 46 pp.

Carder, K.L., R.G. Steward, G.R. Harvey, and P.B. Ortner (1989) Marine humic and fulvic acids: Their effects on remote sensing of ocean chlorophyll. *Limnology and Oceanography*, **34**:68-81.

Feinholz, M.E., S.J. Flora, and J.A. Gashler (1995a) Oceanographic Profiling Observations from the MOBY-L7 Cruise: 25-30 June 1994, Moss Landing Marine Laboratories Technical Publication 95-2, Moss Landing, CA. 46 pp.

Feinholz, M.E., S.J. Flora, and J.A. Gashler (1995b) Oceanographic Profiling Observations from the MOCE-3 Cruise: 27 October to 15 November 1994, Moss Landing Marine Laboratories Technical Publication 95-3, Moss Landing, CA. 94 pp.

Feinholz, M.E. (1996) Relationships between optical and biological properties as modified by physical and chemical variability in the equatorial Pacific ocean. Moss Landing Marine Laboratories Master of Science Thesis, Moss Landing, CA. 79 pp.

Gordon, H.R. and A. Morel (1983) *Remote Assessment of Ocean Color for Interpretation of Satellite Visible Imagery, a Review; Lecture Notes on Coastal and Estuarine Studies, Volume 4.* Springer Verlag, New York. 114 pp.

Kirk, J.T.O. (1983) *Light and Photosynthesis in Aquatic Ecosystems*, Cambridge University Press, New York. 509 pp.

Martin, J.H., G.A. Knauer, W.W. Broenkow, K.W. Bruland, D.M. Karl, L.F. Small, M.W. Silver, and M.W. Gowing (1983) Vertical transport and exchange or materials in the upper waters of the oceans (VERTEX): Introduction to the program, hydrographic conditions, and major component fluxes during VERTEX I. Moss Landing Marine Laboratories Technical Publication 83-2. Moss Landing, CA. 40 pp.

Mitchell, B.G., and O. Holm-Hansen (1991) Bio-optical properties of Antarctic Peninsula waters: differentiation from temperate ocean models. *Deep-Sea Research*, **35**:1009-1028.

Mobley, C.D. (1994) *Light and Water: Radiative Transfer in Natural Waters*, Academic Press, London. 592 pp.

Morel, A. (1988) Optical Modeling of the Upper Ocean in Relation to Its Biogenous Matter Content (Case I Waters). *Journal of Geophysical Research*, **93**:10,749-10,768.

Morel, A. (1991) Light and marine photosynthesis: a spectral model with geochemical and climatological implications. *Progress in Oceanography*, **26**, pp 263.

Morel, A., and L. Prieur (1977) Analysis of variations in ocean color, *Limnology and Oceanography*, **22**:709-722.

Pak, H., D.A. Kiefer, and J.C. Kitchen (1988) Meridional variation in the concentration of chlorophyll and microparticles in the North Pacific Ocean. *Deep-Sea Research*, **35**:1151-1171.

Petzold, T.J. and R.W. Austin (1968) An Underwater Transmissometer for Ocean Survey Work, Visibility Laboratory, University of California, San Diego, S.I.O Ref. 68-9.

Preisendorfer, R.W. (1961) Application of Radiative Transfer Theory to Light Measurements in the Sea, International Union of Geodesy and Geophysics, International Association of Physical Oceanography. Symposium on Radiant Energy in the Sea, Helsinki, 4-5 August 1960. Monograph No. 10.

Preisendorfer, R.W. (1958) Directly obsevable quantities for light fields in natural hydrosols, Visibility Laboratory, University of California, San Diego, S.I.O Ref. 58-46 29 pp.

Prieur, L., and S. Sathyendranath (1981), An optical classification of coastal and oceanic waters based on the specific spectral absorption curves of phytoplankton pigments, dissolved organic matter, and other particulate materials. *Limnology and Oceanography*, **26**:671-689.

Sea-Bird Electronics Inc. (1994) SEASOFT CTD Data Acquisition Software. Sea-Bird Electronics, Inc. 1808 136th Place N.E. Bellevue, WA 98005

Sea Tech Inc. (1994) Transmissometer Manual, Sea Tech Inc. P.O. Box 779 Corvallis OR 97339

Smith, R.C., and K.S. Baker (1981) Optical properties of the clearest natural waters (200-800 nm). *Applied Optics*, **20**:177-184.

Spinrad, R.W., H. Glover, B.B. Ward, L.A. Codispoti and G. Kullenberg (1989) Suspended particle and bacterial maxima in Peruvian coastal waters during a cold water anomaly. *Deep-Sea Research*, **36**:715-733.

University of Maryland (1992) The analysis of carbon and nitrogen from sediments and the particulate fraction of water from estuartine/coastal systems using elemental analysis. University of Maryland Center for Environmental and Estuarine Studies, Chesapeake Biological Laboratory, Solomons, MD.

Van de Hulst, H.C. (1957) *Light Scattering by Small Particles*, John Wiley, New York 470 pp.

Voss, K.J. (1992) A spectral model of the beam attenuation coefficient in the ocean and coastal areas. *Limnology and Oceanography*, **37**:501-509.

Voss, K.J., and R.W. Austin (1993) Beam-attenuation measurement error due to small-angle scattering acceptance. Journal of Atmospheric and Oceanic Technology, **10**:113-121.

Zaneveld, J.R.V., R.W. Spinrad, and R. Bartz (1982) An optical settling tube for the determination of particle size distributions. Marine Geology, **99**:357-376.